# Environmental impact of noble metal radionuclides and their use in nuclear forensics

---

# Umwelteinwirkung von Edelmetallradionukliden und deren Verwendung in der nuklearen Forensik

Von der Fakultät für Mathematik und Physik

der Gottfried Wilhelm Leibniz Universität Hannover

zur Erlangung des akademischen Grades

Doktorin der Naturwissenschaften

Dr. rer. nat.

genehmigte Dissertation von

## M. Sc. Anica Weller

2021

I seem to have been only like a boy playing on the seashore, and diverting myself in now and then finding a smoother pebble or a prettier shell than ordinary, whilst the great ocean of truth lay all undiscovered before me.

(Isaac Newton)

# Acknowledgements

# Abstract

This dissertation focuses on the development of analytical protocols for the measurement of difficult-to-measure noble metal radionuclides and the detection of minute amounts of these nuclides. The noble metal radionuclides of interest were radiosilver $^{108m}$Ag and radiopalladium $^{107}$Pd, which have a considerably long half-life of 438 a and $6.5 \cdot 10^6$ a, respectively. For these studies, a variety of analytical separation and enrichment procedures in combination with radiometric and mass spectrometric methods were employed. The results of these studies are published in three publications.

During previous work, low activity concentrations of the radiosilver isotopes $^{108m}$Ag and $^{110m}$Ag were found in seafood samples from a close proximity of the Fukushima Daiichi NPP. Increased detection limits due to concomitant gamma emitters such as $^{134}$Cs and $^{137}$Cs made the low-level measurements of radiosilver difficult. Nevertheless, the determination of radiosilver after a nuclear accident is of interest as it possibly can give information on the condition of control rods of PWRs or other core components. For this reason, the first publication deals with the development of a fast and precise analytical separation protocol of minute amounts of $^{108m}$Ag in the presence of magnitudes higher concentrations of other gamma emitters. The autodeposition of radiosilver on a copper plate has proven as simple and easily adaptable for almost all laboratories, for aqueous and organic samples. The autodeposition was combined with a subsequent gamma spectrometric measurement with a significantly reduced Compton background. As a further aspect, the fate of freshly deposited radiosilver and –cesium was investigated in various soil matrices. Radiosilver proved to bind strongly with the residual fraction, however, organic compounds can elevate silver's mobility and increasing its bioavailability. In the second publication, a case study of the bioavailability of cesium and silver in edible Shiitake mushrooms was performed. Radiocesium showed a bioaccumulation in the shiitake mushroom and autoradiography revealed that the main $^{137}$Cs activity was concentrated in the hymenium. In contrast, radiosilver was not actively taken up by the fruit body and showed a depletion towards the surrounding substrate. LA-ICP-MS measurements revealed possible sorption effects of silver on the outer parts of the fruit body during its growth. Not only can radiosilver measurements be interfered by other gamma emitters, the stable silver isotope $^{107}$Ag itself can interfere the difficult-to measure long-lived radionuclide $^{107}$Pd. The third publication's main subject was the development of an analytical separation protocol and subsequent ultra-trace ICP-QQQ-MS measurement of scarcely studied radiopalladium isotope $^{107}$Pd. The combination of a Pd extraction with cation exchange resin and Ni Resin and the use of an ICP-QQQ-MS in propane/He gas mode allowed the measurement of sub-ng·kg$^{-1}$ palladium isotope concentration with reduction of major interferences. With the developed method, an enhanced isotopic $^{107}$Pd/$^{105}$Pd ratio could be determined in a Chernobyl cooling pond sediment sample for the first time.

Keywords: Noble metal radionuclides, radiosilver, radiopalladium, ultra-trace analysis, gamma spectrometry, autoradiography, LA-ICP-MS, ICP-QQQ-MS

# Kurzzusammenfassung

Der Schwerpunkt der Dissertation lag auf der Entwicklung von Analysenprotokollen für die schwer nachweisbarer Edelmetallradionuklide und den Nachweis kleinster Mengen dieser Nuklide. Insbesondere wurden Radiosilber $^{108m}$Ag und Radiopalladium $^{107}$Pd untersucht, die beide eine lange Halbwertszeit von 438 a bzw. 6,5·10$^6$ a aufweisen. Für diese Studien wurden verschiedene analytische Trennungs- und Anreicherungsverfahren in Kombination mit radiometrischen und massenspektrometrischen Methoden eingesetzt. Die Ergebnisse dieser Untersuchungen sind in drei Publikationen veröffentlicht.

Bei früheren Arbeiten wurden niedrige Aktivitätskonzentrationen der Radiosilberisotope $^{108m}$Ag und $^{110m}$Ag in Meeresfrüchten aus der Nähe des Kernkraftwerks Fukushima Daiichi gefunden. Erhöhte Nachweisgrenzen aufgrund gleichzeitig vorhandener Gammastrahler wie $^{134}$Cs und $^{137}$Cs erschwerten die Messungen der geringen Mengen an Radiosilber. Dennoch ist die Bestimmung von Radiosilber nach einem nuklearen Unfall von Interesse, da diese möglicherweise Aufschluss über den Zustand von Steuerstäben von DWR oder anderen Kernkomponenten geben können. Aufgrund dessen befasst sich die erste Publikation mit der Entwicklung eines schnellen und präzisen analytischen Protokolls für geringe Aktivitäten an $^{108m}$Ag in Anwesenheit von einem Vielfach erhöhter Konzentration anderer Gammastrahler. Die Autodeposition von Radiosilber auf einem Kupferblech hat sich als einfach durchführbar und leicht anpassbar für wässrige und organische Proben erwiesen. Die Autodeposition wurde mit einer gammaspektrometrischen Messung kombiniert, welche einen deutlich reduzierten Compton-Untergrund zeigte. Als weiterer Aspekt dieser Studie wurde auch der Verbleib von frisch deponiertem Radiosilber und -cäsium in verschiedenen Bodenmatrices untersucht. Es hat sich gezeigt, dass Radiosilber stark in der Residualfraktion gebunden ist, jedoch können organische Verbindungen die Mobilität des Silbers erhöhen und seine Bioverfügbarkeit steigern. In der zweiten Veröffentlichung wurde eine Fallstudie über die Bioverfügbarkeit von Cäsium und Silber in essbaren Shiitake-Pilzen durchgeführt. Radiocäsium zeigte eine Bioakkumulation im Shiitake-Pilz, und die Autoradiographie ergab, dass der größte Anteil der Aktivität von $^{137}$Cs im Hymenium konzentriert war. Im Gegensatz dazu wurde das Radiosilber nicht aktiv vom Fruchtkörper aufgenommen und war verglichen mit dem umgebenen Substrat abgereichert. LA-ICP-MS-Messungen ergaben das mögliche Sorptionseffekte von Silber an den äußeren Teilen des Fruchtkörpers während des Wachstums stattgefunden haben. Die Messung von Radiosilber kann nicht nur durch andere Gammastrahler gestört werden, sondern das stabile Silberisotop $^{107}$Ag selbst kann andere wie z.B. das schwer zu messende langlebige Radionuklid $^{107}$Pd stören. Daher befasste sich die dritte Publikation mit der Methodenentwicklung zur Separation und anschließender ICP-QQQ-MS-Messung von Ultraspuren des wenig untersuchten Radiopalladium-Isotops $^{107}$Pd. Die Kombination einer Pd-Extraktion mit Kationenaustauscherharz und Ni-Harz und anschließender ICP-QQQ-MS Messung im Propan/He-Gas-Modus ermöglichte die Bestimmung von Palladium- Konzentrationen im sub-ng·kg$^{-1}$-Bereich bei gleichzeitiger Reduzierung der wichtigsten Interferenzen. Mit der entwickelten Methode konnte zum ersten Mal ein erhöhtes $^{107}$Pd/$^{105}$Pd-Isotopenverhältnis in einer Sedimentprobe aus dem Kühlteich von Tschernobyl nachgewiesen werden.

Schlagwörter: Edelmetallradionuklide, Radiosilver, Radiopalladium, Ultraspurenanalyse, Gammaspektrometrie, Autoradiographie, LA-ICP-MS, ICP-QQQ-MS

# Contents

# List of abbreviations

| | |
|---|---|
| **BWR** | Boiling water reactor |
| **CANDU** | Canada Deuterium Uranium |
| **CRC** | Collision reaction cell |
| **CTBT** | Comprehensive Nuclear Test Ban Treaty |
| **DMG** | Dimethyl glyoxime |
| **DOM** | Dissolved organic matter |
| **DRC** | Dynamic reaction cell |
| **DU** | Depleted uranium |
| $E_0$ | Standard electrode potential |
| **ETV** | Electrothermal vaporisation |
| **EURT** | East Urals Radioactive Trace |
| **FY** | Thermal neutron fission yield |
| **HEU** | High-enriched uranium |
| **HLW** | High level liquid waste |
| **HPGe** | High-purity germanium |
| **HPLC** | High-performance liquid chromatography |
| **HR** | High resolution |
| **IAEA** | International Atomic Energy Agency |
| **ICP-QMS** | Inductively coupled plasma quadrupole mass spectrometer |
| **ICP-QQQ-MS** | Inductively coupled plasma tripe quadrupole mass spectrometer |
| **INES** | International Nuclear and Radiological Event Scale |
| **LA** | Laserablation |
| **LEU** | Low-enriched uranium |
| **LSC** | Liquid scintillation counter |
| **LWR** | Light water reactor |
| $m/z$ | Mass to charge |
| **MC** | Multicollector |
| **MOX** | Mixed oxide |
| **MS** | Mass spectrometry |
| **NA** | Neutron activation |
| **NPP** | Nuclear Power Plant |
| **NRX** | National Research eXperimental |

| | |
|---|---|
| **PET** | Positron-emission tomography |
| **PGE** | Platinium group elements |
| **PHWR** | Pressurized heavy water reactor |
| **PTBT** | Treaty Banning Nuclear Weapon Tests in the Atmosphere, in Outer Space and Under Water |
| **PUREX** | Plutonium uranium reduction extraction |
| **PWR** | Pressurized water reactor |
| **RBMK** | *reaktor bolshoy moshchnosti kanalnyy,* high-power channel-type reactor |
| **RPV** | Reactor pressure vessel |
| **SIC** | Silver-indium-cadmium |
| $T_{1/2,bio}$ | Biological half-life |
| $T_{1/2,eff}$ | Effective half-life |
| $T_{1/2,phy}$ | Physical half-life |
| **TBP** | Tributyl phosphate |
| **TMI-2** | Three Miles Island Unit 2 |
| **TOF** | Time of flight |
| **TPNW** | Treaty on the Prohibition of Nuclear Weapons |
| **UN** | United Nations |
| **UO$_2$** | Uranium dioxide |
| **VVER** | Water-water energetic reactor |

# Introduction

This cumulative PhD thesis comprises the three following publications. In the next chapters, these publications are put into context with current literature and developments in the analysis of environmental radioactivity and nuclear forensics.

**D1.** A. Weller, D. Zok, S. Reinhard, S. K. Woche, G. Guggenberger, G. Steinhauser; Separation of Ultratraces of Radiosilver from Radiocesium for Environmental Nuclear Forensics, *Anal. Chem.*, 2020, 92, 5249-5257. DOI: 10.1021/acs.analchem.9b05776

**D2.** A. Weller, D. Zok, G. Steinhauser; Uptake and elemental distribution of radiosilver $^{108m}$Ag and radiocesium $^{137}$Cs in shiitake mushrooms (*Lentinula edodes*), *J. Radioanal. Nucl. Chem.*, 2019, 322, 1761-1769. DOI: 10.1007/s10967-019-06778-1

**D3.** A. Weller, T. Ramaker, F. Stäger, T. Blenke, M. Raiwa, Ihor Chyzhevskyi, Serhii Kirieiev, Sergiy Dubchak, G. Steinhauser, Detection of the fission product Palladium-107 in a pond sediment sample from Chernobyl, *Environ. Sci. Technol. Lett.* 2021, 8, 8, 656-661; DOI: 10.1021/acs.estlett.1c00420

# Chapter 1

# Overview

## 1.1 Sources of environmental radioactivity

Natural and anthropogenic radionuclides are ubiquitous in all compartments of the environment. Natural occurring radionuclides include primordial radionuclides (existence since the formation of the earth; for example $^{40}$K, $^{232}$Th, $^{238}$U) or constantly produced radioactive elements. These are decay products of the primordial radionuclides (radiogenic radionuclides e.g. $^{210}$Pb, $^{222}$Rn, $^{234}$U) or build-up nuclides during spallation and nuclear activation processes in the atmosphere (cosmogonic radionuclides, e.g. $^{14}$C, $^{3}$H). Anthropogenic radionuclides are nuclides, which are produced by man-made actions. Major contributors for these anthropogenic radionuclides are nuclear energy production, nuclear weapons explosions, medical radionuclide production, and research facilities.

### 1.1.1 Nuclear fuel cycle

The continuously increasing demand for energy production resulted in the development of nuclear power generation for civil use. Nuclear power generation uses the released energy from nuclear fission of heavy nuclei. In contrast to the uncontrolled – supercritical – nuclear fission chain reactions in nuclear weapons, the nuclear fission in nuclear reactors are self-sustaining – critical – chain reactions, which continuously release energy in form of heat to its surroundings. The heat is used to generate steam, which is used to power turbines for electrical energy generation. The overall process of nuclear power generation from the mining and processing of natural uranium ores, fuel fabrication, use in nuclear power reactors, as well as the reprocessing of the nuclear fuel and/or final repository is called the nuclear fuel cycle (Figure 1). The release of radioactive material from the nuclear fuel cycle into the environment can be manifold.[1, 2]
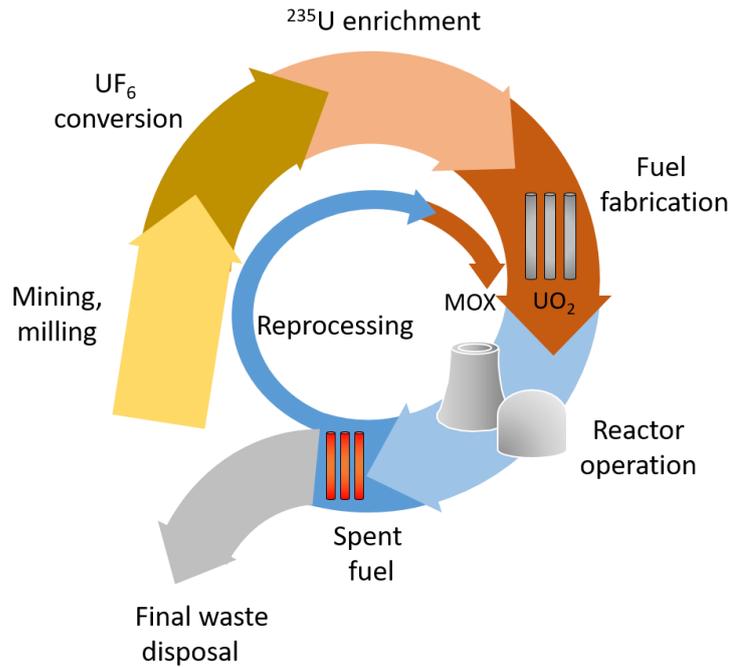
Figure 1: Scheme of the major steps in the nuclear fuel cycle.

The starting point of the nuclear fuel cycle is the mining of ores with a natural isotopic composition of uranium. Natural uranium consists of the isotopes $^{238}U$ (99.28 %), $^{235}U$ (0.71 %), $^{234}U$ (0.005 %) and only traces of $^{233}U$ and $^{236}U$. Only the $^{235}U$ isotope has a significant neutron capture cross section for an induced fission reaction with thermal neutrons and is hence called fissile isotope. In contrast, the isotope $^{238}U$ is prone to neutron capture to $^{239}U$, which consequently further decays to $^{239}Np$ and $^{239}Pu$. The produced $^{239}Pu$ is also a fissile nuclide. The cumulative global uranium production is estimated to a total of 2.3 Mt $U_3O_8$. [3] The total global uranium resources are estimated to 5.5 Mt $U_3O_8$.[3] Depending on the uranium reserve, the mining takes place in an open pit (e.g. Rössing, Namibia; McLean Lake, Canada), by acid in-situ leach (e.g. predominantly: alkaline leaching in USA and acid leaching in Soviet Union) or underground mining (e.g. Olympic Dam, Australia). The average uranium ore grade (mainly triuranium octoxide $U_3O_8$) in resources usually range from 0.02 % (South Africa) with up to 1.1 % (Canada).[3, 4] The mined uranium ores are crushed and shredded in mills and then chemically leached by acid or alkaline solutions. Afterwards the leached uranium is concentrated and purified by solvent extraction, ion-exchange and precipitation.[5] The result of this process is a powder, which is often referred to as 'yellowcake'. The milled $U_3O_8$ can be directly converted to $UO_2$ by reduction with hydrogen for reactors burning on natural uranium fuel such as **Can**ada **D**euterium **U**ranium (CANDU) reactors. Generally, $U_3O_8$ could also be used as fuel material. However, the use of $UO_2$ is preferred due to its higher uranium density, higher thermal conductivity, capability of retaining high amounts of fission products and linear power rating.[6] As an alternative, $U_3O_8$ can be converted in a two-step process from uranium tetrafluoride $UF_4$ to uranium hexafluoride $UF_6$ for enrichment of $^{235}U$. The transformation

13

of uranium to its hexafluoride (boiling temperature: 56.4 °C) offers the opportunity to use isotope enrichment methods, which depend on the gaseous state of the substance. In order to enrich the fissile nuclide $^{235}$U as needed in a low enriched uranium (LEU) to around 2-5 %, the uranium fluoride $UF_6$ undergoes several isotope separation methods such as gas centrifuge and gaseous diffusion. The enriched product (2-5 % $^{235}$U) is later used for fuel fabrication, whereas the majority of the $UF_6$ (~96 %) incurred as depleted uranium (DU). After the $^{235}$U enrichment to the desired degree, the $UF_6$ is re-converted to $UO_2$. The resulting powder is thereafter pressed into pellet form and sintered for hardening and to create ceramic pellets. These fuel pellets are then stacked in rods. The rods or claddings consist of corrosion-resistant metal alloys such as stainless steel or zirconium alloy. In light water reactors (LWR), the fuel rods are filled with helium at 15 to 30 bar. The sealed rods serve as the containment for the radionuclides inside. The fuel rods can be bundled – as specified for boiling water reactors (BWR) and pressurized water reactors (PWR) – into fuel assemblies. The manufactured fuel rods or assemblies are then distributed to the nuclear power plants (NPP).[1]

The fuel assemblies are loaded into the reactor core – often in a hexagonal array of cells. The cell arrays are periodically filled with fuel assemblies and control rods. Most nuclear reactors use water as neutron moderator, coolant, and for heat transportation. After the fuel loading, the reactor can be started and is then operated under criticality (self-sustaining nuclear reactions). The fissile amount of the nuclear fuel burns up within operation time and the fissile $^{239}$Pu is continuously bred. After around half of the operation time, a majority of the fission reactions take place from $^{239}$Pu. During operation, the amount of fission products inside the nuclear fuel rods increases, leading to a subsequent "poisoning" of the reactor. For these reasons, the fuel assemblies need to be replaced after a certain time of operation (e.g. PWR: 3-5 years). Due to heterogeneous neutron flux densities in the cell, the fuel needs to be replaced one after the other by their burn-up. The common reactors types PWR, water-water energetic reactor (VVER), BWR, pressurized heavy water reactors (PHWR e.g. CANDU) and graphite moderated light water cooled reactor (high-power channel-type reactor (RBMK)) have different reactor designs. By using isolable pressure tubes in their reactor designs, the fuel of RBMK reactors can be replaced during operation. In contrast, VVER, PWR and BWR have one reactor pressure vessel, which holds the reactor core with all fuel assemblies. For this reason, the reactors need to shut-down and cool-down for a required time period before the reactor core can be refueled. The spent nuclear fuel is highly radioactive and due to the heat generation from on-going decay of the contained residual radioactive products, the spent fuel needs to be continuously cooled and shielded. The spent fuel is generally stored at site in spent nuclear fuel pools or common nuclear storage facilities for 2 to 5 years. After the storage time, the spent nuclear fuel can either be reprocessed in nuclear reprocessing facilities or as an alternative the nuclear waste needs to be transmuted or disposed of.[1]

Spent nuclear fuel contains amounts of the initial fissile $^{235}U$ and the bred $^{239}Pu$, as well as high quantities of a wide spectrum of fission and neutron activation products. The uranium and plutonium is extracted from spent nuclear fuel during reprocessing and reused in the nuclear fuel cycle, e.g. as mixed oxide (MOX) fuel. The MOX fuel is a blend of reprocessed uranium and plutonium, which is brought to the needed enrichment degree by depleted uranium. In most civil reprocessing facilities (e.g. in Sellafield, UK and La Hague, France) uranium and plutonium are chemically extracted by the PUREX (**P**lutonium **Ur**anium reduction **Ex**traction) process. The PUREX process is based on liquid-liquid extraction of spent nuclear solution in nitric acid media with an organic complexing agent tributyl phosphate (TBP) in the solvent kerosene. The uranium and plutonium ions, together with the nitrate ions, form TBP complexes, which are extracted into the organic phase. The majority of the fission products remain in the nitric acid solution (PUREX raffinate) and are called high-level liquid waste (HLW). The radionuclides of the HLW can be chemically bound through glass vitrification and disposed of. There have been experiments to reduce the radioactive waste of the HLW – especially actinides and long-lived fission products – via transmutation by photon or fast neutron irradiation to generate short-lived or stable isotopes. However, the transmutation is currently not commercially performed and needs further research. Due to high public concern, many states do not perform or commission any reprocessing activities anymore.[1]

The radioactive waste resulting from NPPs as spent nuclear fuel or process waste in glass caskets from vitrification needs to be disposed of. The radioactive waste needs to be stored or disposed safely from external influences (danger of nuclear proliferation, natural catastrophes) and the permeation of radioactive material into the biosphere. The disposal area should withstand major environmental events such as earthquakes, erosion, water leakages for over a time period of several million years due to the long half-live of several radionuclides. Currently only a few states (e.g. Finland, Sweden) have chosen a site for final repository of nuclear wastes (e.g. FIN: spent nuclear fuel, SWE: intermediate operational waste). Other states are still in search for a suitable location of all levels of nuclear waste and therefore need to interim storage their nuclear waste in appropriate facilities. Most states prefer a final repository in national deep geological formations.[1]

Generally, the contribution from nuclear fuel cycles for the effective dose of the population is small. However, local releases from accidents sites such as Chernobyl NPP or Fukushima NPP lead to elevated dose levels. The calculated dose during a 100 year operation of all nuclear power plant facilities is 0.2 µSv per year per caput dose.[7]

The utilization of nuclear power for energy and/or plutonium production led to several incidents with uncontrolled releases of radioactive substances into the environment. The cause and consequences for each release varied in gravity; however, the cause could often be affiliated with a mixture of material, construction and operation errors. The main consequences in form of radioactive contaminations are often local. Yet

radioactive releases, especially air-borne releases can commonly be measured in international monitoring stations.[2, 8]

The International Nuclear and Radiological Event Scale (INES, Figure 2) is an internationally recognized scale for the impact of a nuclear event and was introduced by the International Atomic Energy Agency (IAEA) in 1990. The INES scale categorizes a nuclear event into different severities ranging from 0 to 7. With each section the radiological impact increases on a logarithmic scale. An INES event classified 0 is a deviation of the normal routine operation, however, with overall no safety risk. The classification 1 to 3 are used for incidents with low impact on the environment or humanity. At an event with the scale 4 to 7, the event is classified as a nuclear accident with increasing effects on the environment and humanity. [9]
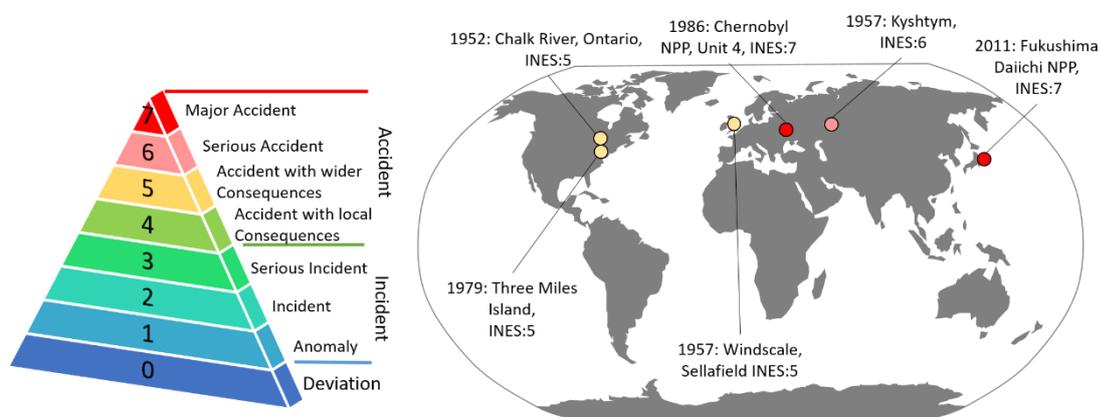


Figure 2: Left site: International Nuclear and Radiological Event Scale (INES). The INES scale is divided into sections 0 to 7 with each higher section indicating a nuclear event with a magnitude higher radiological impact. (Modified after:[9]) Right site: Major nuclear accidents listed INES 5 or higher.

The following accidents with major releases of radioactive substances into the environment classified of INES level 5 or above are chronically and briefly described in the following section and the location presented in Figure 2.

- 1952: On the 12th December the first accident of a thermal reactor took place with a partial core melting, which occurred at the NRX (**N**ational **R**esearch e**X**perimental) heavy-water research reactor at Chalk River Laboratories, Ontario, Canada. The accident was later classified at INES scale of 5 as a nuclear accident with wider consequences. The Chalk River accident occurred after mechanical defects and operation errors during experiments on low power of the 30 MW reactor, which induced a power surge. The experiment was carried out for reactivity measurements. For the experiment, some of the natural uranium rods were operated at low power and lower cooling water flow. During the ramp of the reactor, more control rods –consisting of boron – were raised than allowed in protocol for start-off, which led to a constant increase in power-level. It was attempted to stop the reactor's criticality by dropping the control rods. However, due to a mechanical defect, some control rods could not be lowered fast enough and the power-level further increased. For this reason, the moderator (heavy

water) was dumped into the storage tank, which ceased the criticality. The power-level is estimated to have increased to 100 MW during the 60 s power surge. Due to the lowered cooling rate of the uranium rods, the aluminum cladding as well as the uranium melted and the surrounding water evaporated. The air tubing burst due to hydrogen explosions. An estimated of 0.37 PBq of fission products (majority were short-lived radionuclides) leaked with the cooling water into the basement and the melted uranium was caught in the reactor core. 1000 m$^3$ of the contaminated cooling water was directly released into the Ottowa River, whereas another 3000 m$^3$ were disposed of into the ground of a waste disposal area. [10, 11]

- 1957: The Kyshtym accident occurred on the 29th September in 1957 in the southern Urals in the former Soviet Union at the Mayak reprocessing plant, which primarily was used for the extraction of weapon-grade plutonium. Due to loss of cooling of a HLW storage tank, fission products were released during a chemical explosion. The chemical explosion arose from a storage of nitrate-acetate solution of HLW. On account of predominant politics during this time period the accident as well as the consequences were not reported internationally. Later estimations concluded a release of around 740 PBq of fission products, from which 10 % was dispersed into the atmosphere and the remaining 90 % was released into the nearby environment (forests, grassland, aquatic systems) in form of particles.[12–14] The radioactive plume stretched 300 km into the northeastern region of Mayak and the contamination got the name East Urals Radioactive Trace (EURT).[15] The approximately 1 year old HLW contained mainly fission products such as $^{95}$Zr, $^{144}$Ce, $^{106}$Ru, $^{90}$Sr, and a depletion of $^{137}$Cs. Shortly after the accident, the total radioactive contamination at the Mayak site is estimated to 1-20 PBq·m$^{-2}$. Given the longer half-life of $^{90}$Sr (29 a), the major contamination currently originates from the strontium isotope. The $^{90}$Sr deposition close to the reprocessing plant Mayak reached up to 74 MBq·m$^{-2}$. After 7-14 days following the accident, close settlements with high external exposure were evacuated. An estimated 38,500 people participated in the emergency management and clean up. The Kyshytm or Mayak accident was later classified at the second highest INES rating of 6.

- 1957: Shortly after the Kyshytm accident, another accident transpired at the Windscale nuclear complex in Sellafield on the morning of the 10th October. The accident occurred in one of the two Pile reactors (No. 1), which were used for plutonium production. The reactor used natural and slightly enriched uranium and was moderated by graphite and used air-cooling of the core. The graphite moderator is prone to accumulate Wigner energy (potential energy from dislocation of carbon atoms in the crystal structure through neutron irradiation). As uncontrolled release of Wigner energy could lead to core heating, hence the moderator needs to be annealed by heating at low power and reduced air flows of

17

the nuclear reactor. During the annealing process, the reactor core of No.1 Pile reactor overheated and the graphite moderator as well as part of the fuel caught fire in the air coolant flow. The fire transported an estimated of 1 % of the core into the atmosphere. About 18.6 PBq of fission (especially radioiodine) and neutron activation products and smaller percentages of actinides were released into the environment. The fire at the Windscale Pile reactor was later listed as INES 5 from the IAEA.[12, 16]

- 1979: On the 28th March, a partial core meltdown occurred in the NPP Three Miles Island Nuclear Generating Station Unit 2 with high releases of radioactive gases and fission products. This accident was classified as INES 5. The main cooling system of the PWR reactor Unit 2 malfunctioned, causing the feedwater pumps to shut down. Due to the ceasing feedwater of the secondary loop, the heat and pressure of the primary coolant loop and inside the reactor core increased rapidly, which caused an emergency shut-down of the nuclear chain reaction by inserting all control rods. The residual decay heat needs to be constantly removed from the reactor core to avoid overheating. In the case, that the primary cooling cycle does not obtain sufficient cooling of the reactor, emergency cooling pumps are activated. However, during routine maintenance necessary valves of the auxiliary cooling pumps were closed, leading to an overpressured reactor core. Operators triggered a pressure relief valve, which afterwards did not close accordingly, leading to loss of cooling water in the primary cooling system. The loss-of-cooling accident left the reactor core partially uncovered, which led to a meltdown of the nuclear fuel and zirconium alloy fuel cladding. The destruction of the fuel rods resulted into high releases of radioactivity from the leaked cooling water and airborne releases. An estimated amount of 1.6 PBq of radioactive noble gases and 0.7 TBq radioiodine were released. [17]

- 1986: The accident in the Chernobyl NPP Unit 4 on the 26th April is known as the worst nuclear accident in history and is reported at the highest INES rating at 7. A technical and postponed test at the RBMK reactor type at low power led to an unnoticed xenon-poisoning of the reactor core. Xenon-poisoning occurs in the presence of the highly neutron absorbing fission product $^{135}$Xe. During routine operation, the xenon isotope is constantly burned. However, at low power operation or shut-down of the reactor, $^{135}$Xe is built-up in the reactor and reacts as a neutron poison. For this reason, a reactor cannot be started shortly after shut-down, but needs to wait for the decay of the $^{135}$Xe isotope with a half-life of around 9 hours. As a result of the xenon-poisoning, the power outage during the low power operation dropped to almost zero, and as a consequence the operators lifted an inadmissible amount of control rods from the core. This led to unstable reactor conditions in combination with a positive void coefficient, which led to a subsequent power excursion. The power excursion could not be stopped and was exacerbated by the design of the control rods (graphite tip), which were inserted

at the belated emergency shut-down. The power excursion resulted in a steam explosion triggered by the melting fuel and fuel cladding leaving the core open to the atmosphere. The open core ignited the graphite moderator leading to a fire burning for several days and transporting radioactive material to great heights, contaminating large areas.[18] The release and deposition of volatile radionuclides such as $^{137}$Cs, $^{131}$I could be measured all over Europe. Furthermore, lesser volatile radionuclides such as $^{90}$Sr, U and transuranium elements were deposited regionally around the NPP with major contamination located in Belarus, Ukraine and the Russian Federation. Especially uranium and transuranium elements were emitted in form of fuel particles during explosion and the day-long graphite fire. It is estimated that 5300 PBq (exluding noble gases) were released during the accident in Unit 4 and also up to 1.5 % of the core inventory of refractory radionuclides. The local population and operational forces received a significant radiation dose with several radiation related fatalities, whereas the European region and the Northern Hemisphere population received less than 50 % of the natural background radiation dose.

- 2011: The second nuclear accident, which was classified at the highest INES level of 7 was the accident on the 11$^{th}$ March 2011 on the Fukushima Daiichi NPP complex, which included Units 1-4. After a recorded earthquake of the magnitude of 9 in the coastal region in close proximity to Japan, a subsequent tsunami struck the main island Honshu. The BWR reactor Units 1-3 followed protocol with an emergency shutdown of the running reactors. Unit 4-6 were at revision at this time and not in operation. After emergency shutdown, the reactor core needs continuous cooling of the decay heat, which is around 1 % of the initial thermal power. Due to the damage of the external grid, the power for the cooling water pumps could not be taken from the grid. For this reason, emergency diesel generators were started, which can provide enough power to enable sufficient cooling for several days. However, around 40 min after the earthquake the Japanese coast was struck by a tsunami. The tsunami with a height of 14 m was higher than the tsunami protection walls, flooded and destroyed the emergency diesel generators. As a result, emergency batteries and power independent cooling mechanism were engaged. These mechanisms could only provide power and cooling for a limited amount of time. As the cooling of the core was slowly lost, the pressure and temperature rose inside the reactor subsequently leading to melting of the nuclear fuel and cladding. The reaction of the zirconium alloy cladding with water at temperatures of 1000 °C led to the generation of hydrogen and furthermore to several hydrogen explosions at Unit 1, 3 and 4 (and presumably 2), which released radionuclides into the environment. Moreover, several water leakages from the core and outside emergency cooling operations released activities. During the NPP accident at the Fukushima Daiichi power station around 520 PBq of predominantly volatile radionuclides were released into

the environment. A 30 km radius around the NPP was evacuated and declared as restricted area.[18, 19]

In conclusion, throughout the history of nuclear power generation, several incidents and accidents occurred independent of the reactor type or reprocessing facility, often as a combined result of operational, construction and mechanical errors in spite of generally redundant safety features in NPPs. The different accident scenarios led to uncontrolled releases of various radionuclides into the environment, which ecological fate is determined by the physical and chemical properties of the isotope.

### 1.1.2 Nuclear weapons explosions

Historically, the focus was not only on the civil use of nuclear energy, but also major efforts were put into the development of nuclear weapons for military purposes. Due to the high density of potential energy released from nuclear fission from highly enriched fissile radionuclides such as $^{235}$U and $^{239}$Pu, nuclear weapons hold a much higher destructive effectiveness than conventional weaponry. The United States of America (US) developed the first nuclear weapon as part of the Manhattan Project and the first nuclear detonation took place at the Trinity test site. The bombing of the Japanese cities Hiroshima and Nagasaki was the first use of nuclear weapons in warfare (World War II). After the World War II, the Cold War led to a nuclear arms race between the US and the Soviet Union. Furthermore, other nations such as France, Great Britain, China, and India pursued their own nuclear weapons programs. In result, the newer developments and dimensions of the nuclear weapons (fission, thermonuclear bombs) were frequently tested, mainly in the atmosphere, under water and underground. The atmospheric nuclear weapon detonations are the main source for the high global dispersal of anthropogenic radionuclides in the Northern and Southern atmosphere resulting in man-made radiation exposure.[7] Due to the self-inflicted increased radiation exposure, some of the nations in possession of nuclear weapons signed and ratified in 1963 the *Treaty Banning Nuclear Weapon Tests in the Atmosphere, in Outer Space and Under Water (abbreviated as: Partial Test Ban Treaty, PTBT)*. The treaty solely allowed underground testing of nuclear weapons. The relocation of the nuclear weapons testing showed an effective decrease in released radionuclide activities in the Northern and Southern Hemisphere in the subsequent years of the PTBT, which led to the so-called 'bomb peak' at 1963-1965 with a continuing declining trend correlating with the half-life of the emitted radionuclides. The emissions from nuclear weapons testing were not reduced to zero, but continued more locally at underground testing, or by nations not signing the PTBT e.g. France and China in atmospheric releases. After the end of the Cold War in 1991 and with nuclear disarmament in mind, further negotiations for a complete ban of nuclear weapons testing were supported by the United Nations (UN) General Assembly, which consequently led to the development of the *Comprehensive Nuclear-Test-Ban Treaty* (CTBT). The CTBT was then adopted by the UN General Assembly in 1996 and initially signed by 71 states. Some states in possession of nuclear weapons have signed the treaty but did not ratify it,

namely China, and the US, further nuclear states India, Pakistan and North Korea did not sign the treaty. In 2017, the UN General Assembly adopted the *Treaty on the Prohibition of Nuclear Weapons (TPNW)*. The TPNW demands the elimination of all nuclear weapons starting from the development process up to successful dismantling of existing nuclear weapons. The several nuclear weapons explosions hold major contribution to the worldwide collective dose in 1945-1980 from ionizing radiation. The dose was retrospectively estimated from $^{90}$Sr and $^{137}$Cs releases during the bomb years and data from the numbers and yields for the nuclear weapons, as well as an empirical atmospheric transport model. The world average annual effective dose was estimated to 150 µSv in 1963, which decreased over the years to 5 µSv in 2000 (mainly $^{14}$C, $^{90}$Sr and $^{137}$Cs). The dose is reported to be 10 % higher in the Northern Hemisphere than in the Southern Hemisphere owing to the location of testing sites and hemispheric transport model.[7]

### 1.1.3 Other radionuclide sources

Another major source for radionuclides in the environment is the production and application of radioisotopes in medicine. Radiotherapy for cancer and other illness treatment utilizes various different radioisotopes. Generally, short-lived radioisotopes of elements with very specific binding properties in different body parts are favorable. Typical radionuclides are $^{131}$I for whole-body scintigraphy or $^{99m}$Tc for hexakis scintigraphy. The use of fluorinated desoxyglucose with the positron emitter $^{18}$F is used in positron-emission tomography (PET).[20] Depending on the medical application, different types of ionizing radiation are used in dependence on their physical properties such as gamma rays for imaging purposes and pure betas and alphas for irradiation of unwanted cell structures. The production of medical radioisotopes is often performed in cyclotrons, synchrotrons, accelerators, or nuclear reactors.[21, 22] Due to the general short half-life of these isotopes, long transport ways are disadvantageous and medicine facilities often have their own production equipment, however, some radioisotopes can only be produced at selected nuclear reactors in the needed quality and quantity. The production often produces longer-lived byproducts, which are in need of adequate waste disposal.[23]

Furthermore, anthropogenic radionuclides are produced in research facilities and industry for selected applications. Other sources for radionuclides are the energy production from burning coal and the production of natural gas. Hereby, natural radionuclides from reservoirs are released accelerated into the environment by the mining and processing activities. Major radionuclides are uranium and thorium, as well as their daughter nuclides.[24, 25]

### 1.2 Ecological fate

Generally, radionuclides behave similarly as the respective stable isotopes of the same element in the environment.[26] The environment consists of four compartments: the lithosphere, hydrosphere, biosphere, and atmosphere, which are continuously

interacting in several interrelationships. Matter and energy are constantly transported into and between the compartments in various physical, chemical and biological processes. The field of ecology focuses on the intra- and interaction of the biosphere with the other compartments and focuses on the organisms. These organisms form a so-called ecosystem with the surrounding environment and resources. The specialized field of radioecology investigates the fate of radionuclides in the environment with focus on the radiation exposure of humans. Humans are prone to the exposure of radionuclides and ionizing radiation from internal and external sources. External radiation exposure comes from natural and anthropogenic radionuclides present in the soil, water and air. In contrast, internal exposure of humans originates from the incorporation of radionuclides via two main pathways: the ingestion via the food chain and the inhalation of radioactive gases and respirable aerosols and particles. The radionuclides are transported in and along the environmental compartments and along the food chain as the respective stable isotopes and can be similarly used by the organisms in their metabolism. Along the food chain, the uptake of radionuclides from soil to plant, (to animal), and to the human can be described by various transfer factors, which describe the metabolistic activity of the radionuclide towards the following chain link. In this relationship the human being is generally assumed to be the last link in the chain. The intake of specific radionuclides leads to incorporation into the human body and possibly long dwell times in the corresponding human organ. The dwell time of the radionuclide in an organ can be described by the effective half-life $T_{1/2,\text{eff}}$, which takes the biological half-life $T_{1/2,\text{bio}}$ and physical half-life $T_{1/2,\text{phy}}$ into consideration. The biological half-life is the time in which half of the incorporated amount of the element is excreted from the body. The physical half-life is the time in which half of the amount of radionuclides is decayed. [27, 28]

During accidental releases from e.g. a NPP failure, as schematically presented in Figure 3, three major pathways into the environment are distinguished: a) fallout or dry deposition of airborne radionuclides, b) washout or wet deposition of air-borne radionuclides during precipitation as particles or chemical compounds and c) leakage of contaminated water from the reactor buildings. After the release, the emitted radionuclides are distributed in the compartments and the food chain. The distribution needs different time intervals depending on the media (with decreasing distribution efficiency: air, water or soil) and the type of radionuclides (e.g. volatility and absorption efficiency). Whereas natural radioactivity without human activities is generally in equilibrium within the environmental compartments, releases of anthropogenic radionuclides in relatively to the age of the earth short time intervals are often in disequilibrium. Such a disequilibrium results in locally increased radiation exposure from external and internal sources.[27]
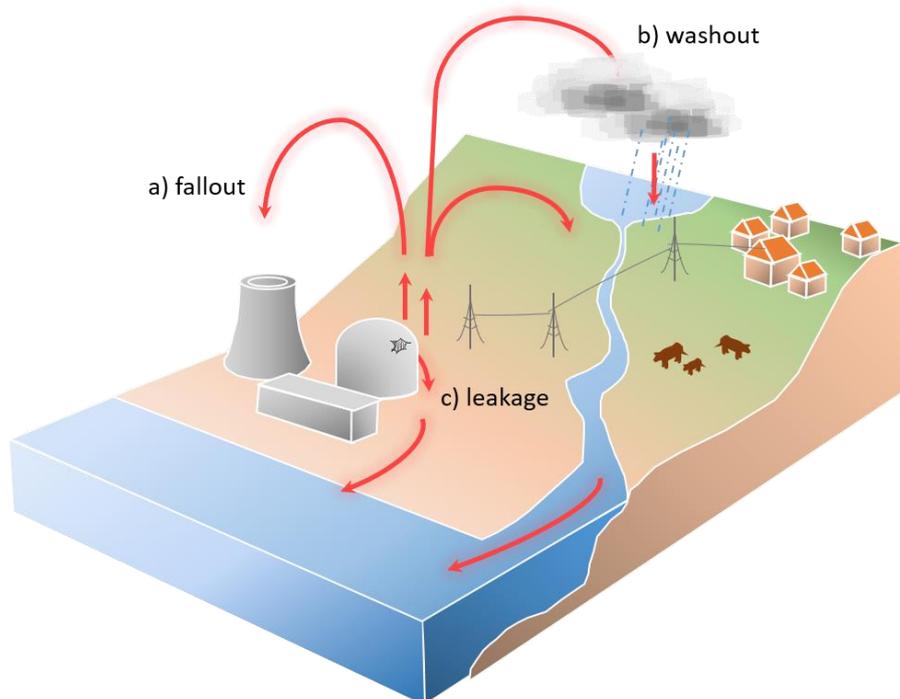
Figure 3: Pathway of radionuclide releases during a nuclear power plant accident. a) Fallout and dry deposition of air particle bound radionuclides, b) washout and wet deposition of air released radionuclides-either particle-bound or as a chemical compound during precipitation, c) water leakage from the reactor building.

Additionally, the slightly different behavior of isotopes of the same element in nature should be taken into consideration. Due to slightly changed physical properties resulting from the mass differences of the different isotopes mass fractionation is noticeable in the environment. This effect ranges from physical processes such as evaporation to biochemical processes. This is especially visible with lighter elements, where the relative mass differences of the isotopes are high. However, it is also recognizable for heavy nuclei and can be used for isotope fractionating as needed for enrichment processes

### 1.3 Nuclear forensics

Nuclear forensics is used for source appointment of radioactive releases, as well as trafficking of nuclear material and unauthorized enrichment. As the environmental pollution from releases of radioactivity are often enormous and pose health risk for humans and in case of nuclear accidents involves a comprehensive cleanup of contaminated areas at great costs, the evidence of the source needs to be certain. Environmental nuclear forensics can also be used for the understanding of current countermeasures as well as the evolution of a nuclear accident, which enables an adequate adaptation of safety features for other existing and future NPPs, and an accurate situation report, which allows adequate decommissioning. The types and amount of radionuclides produced by nuclear weapons, nuclear reactors, enrichment and reprocessing facilities vary due to different nuclear reactions and process steps. For this reason, each event leaves a fingerprint, which can be analyzed with a combination of chronometry and radiochemistry taking into account existing data sets from literature and calculations. Chronometry takes advantage of the different half-lives of radionuclides, which allows

the determination of the age of radioactive material with isotope dating techniques as well as parent-daughter ingrowth. Radiochemistry is applied on the radioactive material for further insight. The radioactive material is chemically separated to reduce interferences from other radionuclides and to allow low-level measurements of small amounts of material. Typically, in radiochemistry, precipitation, complexation, and ion exchange are the means of choice for separation followed by measurement with radiometric or mass spectrometric methods. Radiometric methods analyze the radioactive decay of radionuclides. Due to the different types of radiation, different radiometric measurements are employed for e.g. alpha, beta and gamma measurements via proportional counters, liquid scintillation counting (LSC), and semiconductor detectors. Radiometric methods are especially favorable for short-lived radionuclides, which allows the detection of minute amounts of ionizing radiation. For long-lived and stable nuclides, mass spectrometric methods are often used to achieve lower detection limits as well as shorter measurement times for the nuclides. [26, 29]

The radionuclide profile varies from the source of the radioactive material. Radionuclides released from nuclear weapons explosion show a different profile from radionuclides produced in civilian nuclear reactors. During nuclear weapons explosions, the nuclear chain reaction is uncontrolled, building-up a very short and very high neutron flux density at the time of explosion. For this reason, the majority of the released radionuclides are fission products and initial fissile radionuclides ($^{235}$U, $^{239}$Pu), because the duration of the neutron flux does not allow to produce secondary neutron activation products from fission products or other activation products. In contrast, in a nuclear reactor, the nuclear chain reaction is critical and the neutron flux density is kept controlled throughout the fuel. The fuel is used for 3-5 years, which enables a continuous production of neutron activation products of the fuel and fission products inside. For this reason, also typical secondary neutron activation products as $^{134}$Cs are found in spent nuclear fuel.[29]

The radionuclide profile in spent nuclear fuel is further dependent from the enrichment degree, the fuel material (UO$_2$, MOX), the reactor type (PWR, BWR, RMBK, CANDU) and the reactor operation (reactor shut-downs, burn-up). Many civilian reactors are LWRs, which operate on LEU with an enrichment degree of 2-5 % $^{235}$U. Reactors operating with graphite moderator and/or heavy water need a lesser degree of enrichment or can operate on natural uranium fuel, which is generally used in the chemical form of oxide due to chemical and temperature stability. Some reactor types allow the use of MOX fuel after adjustment of the neutron fluxes, which is often combined with UO$_2$ fuel assemblies in the cores. By a known history of the nuclear fuel, an accurate radionuclide profile can be calculated. For the burn-up and fuel composition calculation, data from

24

post-irradiation examination of spent nuclear fuel is utilized. Fresh nuclear fuel is generally based on $UO_2$, which crystallizes in a cubic fluorite crystal structure (Figure 4).
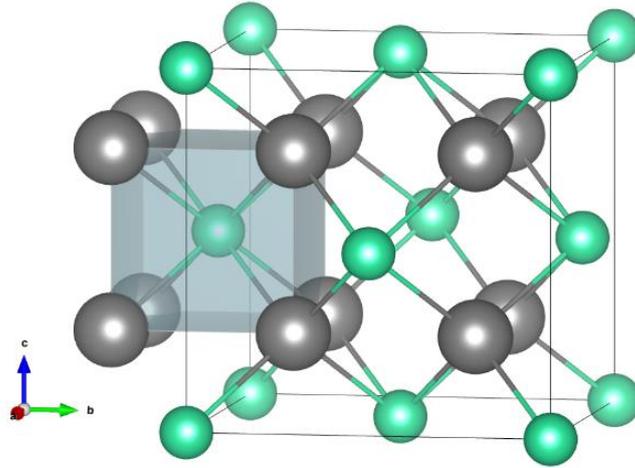


Figure 4: Cubic fluorite crystal structure of $UO_2$. In grey $O^{2-}$ and in green $U^{4+}$.[30, 31]

The $UO_2$ fuel has a high stability during operation against temperature and chemical influences, but has a poor thermal conductivity, which leads to uneven temperature profiles and thermal expansion of the fuel during irradiation. During irradiation, the stoichiometry of the fuel changes with continuing nuclear reactions, burn-up and temperature. This change in stoichiometry leads to alteration of material properties and eventually can cause fuel cracking and fission gas releases inside the cladding. A variety of fission products accumulate between the fuel and zirconium alloy cladding, but it is also known that in spent nuclear fuel additional fission product phases are built up. Such phases can be composed of metal nanoparticles containing molybdenum, ruthenium, rhodium, silver, and palladium in hexagonal structure or of barium strontium zirconate in cubic perovskite structure.[32] The radionuclide profile as well as the chemical form can be diverse in spent nuclear fuel and requires extensive studies to assess. Pfeiffer *et al.* calculated the radionuclide content in tons of heavy metal for $UO_2$ and MOX of spent nuclear fuel for German nuclear reactors of the types PWR, BWR and VVER.[33] The activity concentration of spent uranium dioxide ($UO_2$) nuclear fuel of a pressurized nuclear reactor (PWR) with a 55 GWd burn-up with data taken from Pfeiffer *et al.* is presented in Figure 5.[33] The activity concentration of several long-lived fission products, neutron activation products and actinides are shown in dependence of the years after unloading of the spent nuclear fuel in correlation to the total activity concentration over all radionuclides present in the fuel. After the cool-down period of 2-5 years in spent fuel pools, the majority of the short-lived radionuclides have decayed and the total activity is dominated by medium long-lived radionuclides such as $^{90}Sr$, $^{137}Cs$ and $^{241}Pu$. After longer time periods of above 1000 years in suitable storage capabilities such as final repositories, the total activity is determined by long-lived fission products and actinides. For safety assessments of final repositories, among other things, intermediate and long-lived radionuclides need to be taken into consideration from a radiation exposure and ecological point of view.

25
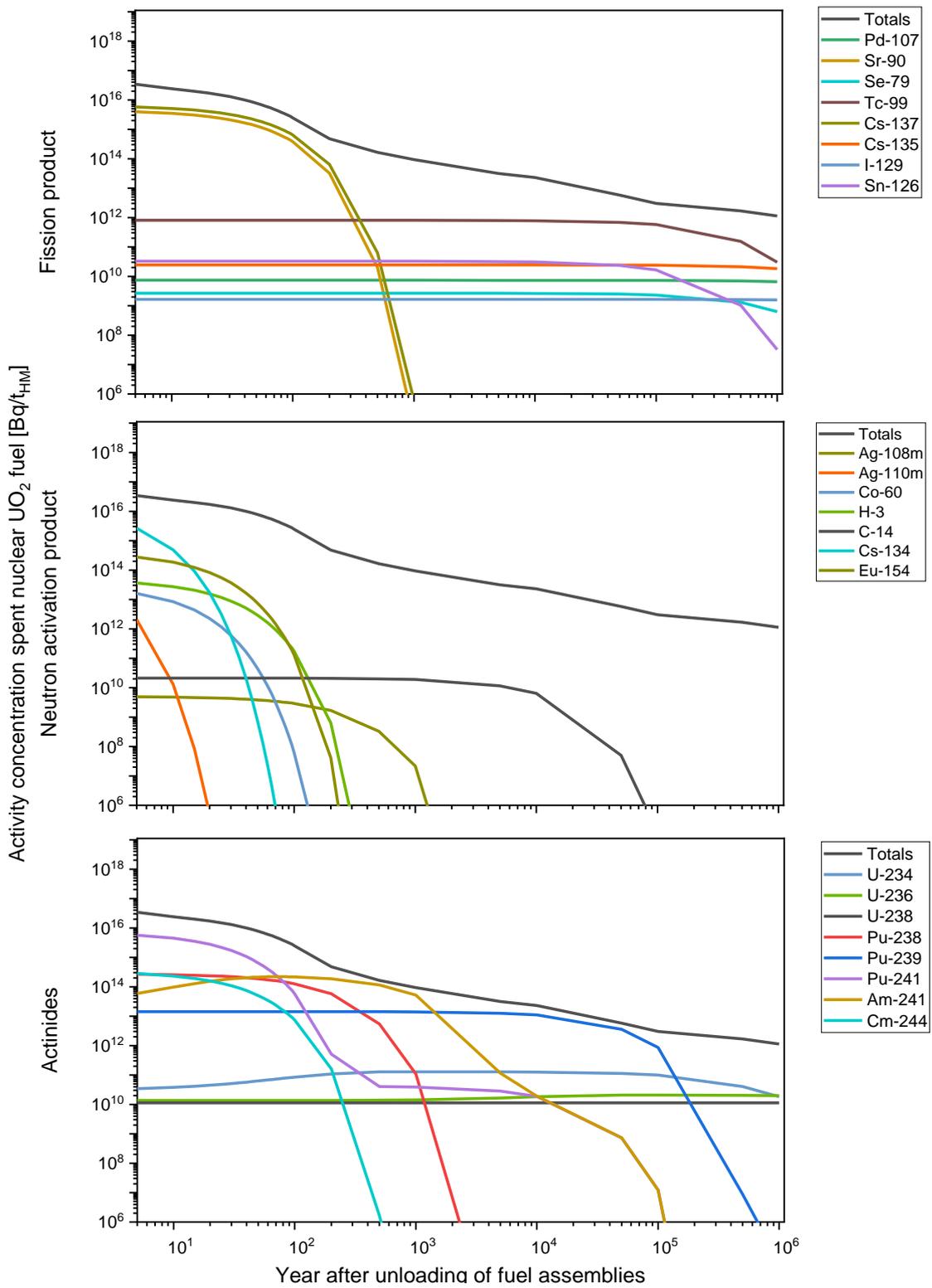
Figure 5: Activity concentration of several fission products, neutron activation products and actinides in UO₂ spent nuclear fuel of a PWR with a burn-up of 55 GWd. The total activity concentration is the activity of all radionuclides present in the fuel. Data is taken from Pfeiffer *et al.*[33].

In addition, not only the spent nuclear fuel can be a source for radioactive releases of for example a pressurized water reactor (Figure 6). A reactor consists of several more components as the reactor pressure vessel (RPV), control rods, concrete bioshield, and

moderator media (mostly water), which a prone to constant neutron activation (NA) due to the closeness to the reactor core with high neutron fluxes present. A further source of radionuclides in reactors are corrosion products. The corrosion products are produced by dissolving products from construction materials (mainly steel components), which are transported in the primary circuit into the core and are activated. Afterwards, the activated corrosion products are transported and deposited inside the primary circuit. [34] Typical longer-lived radionuclides found after operation of a NPP are summarized in Table 1.

Table 1: Typical medium and long-lived radionuclides found in a PWR after operation. NA: Neutron activation, FP: fission products.

| Cross-section of a PWR | Sources in a NPP | Typical medium and long-lived radionuclides |
|---|---|---|
|  Figure 6: Schematic cross-section of a pressurized water reactor (PWR). | Nuclear fuel | Enriched $UO_2$ (PWR: 3.5 % $^{235}U$), MOX |
| | NA actinides | $^{236}U$, $^{237}Np$, $^{238}Pu$, $^{239}Pu$, $^{240}Pu$, $^{241}Pu$, $^{241}Am$ |
| | FP of $^{235}U$ | $^{79}Se$, $^{90}Sr$, $^{93}Zr$, $^{95}Zr$, $^{99}Tc$, $^{107}Pd$, $^{126}Sn$, $^{129}I$, $^{135}Cs$, $^{137}Cs$, $^{147}Pm$, $^{151}Sm$ |
| | NA steel components | $^{55}Fe$, $^{59}Ni$, $^{63}Ni$, $^{60}Co$, $^{93}Zr$, $^{94}Nb$ |
| | NA control rods | $^{108m}Ag$, $^{60}Co$ |
| | NA concrete bioshield | $^{3}H$, $^{152}Eu$, $^{41}Ca$ |
| | NA moderator media | $^{3}H$ |

As the processes of radionuclide production vary depending on the source, the use of isotopic ratios often allows a source assignment. If possible, it is favorable to use different isotopes of the same element, because the isotopes behave almost the same during the release processes and in the environment. A typical example is the use of radiocesium isotopes $^{134}Cs$, $^{135}Cs$, and $^{137}Cs$, which show similar element specific behavior in the environment, however are all produced differently:

- $^{134}Cs$ as a secondary neutron activation product of $^{133}Cs$, produced almost only in nuclear reactors with constant neutron fluxes.
- $^{135}Cs$ is predominantly produced during shut-down of reactors from decay of highly neutron absorbing radionuclide $^{135}Xe$ and during nuclear weapons explosion.
- $^{137}Cs$ as a prominent fission product produced by nuclear fission of heavy nuclei.

The use of radiocesium isotopic ratios allows statements on the production pathways in nuclear weapons or different type of reactors: $^{135}Cs/^{137}Cs$(Nuclear weapons):≈2.0-2.7; $^{135}Cs/^{137}Cs$(Chernobyl):≈0.5; $^{135}Cs/^{137}Cs$(Fukushima):≈0.35, (all ratios decay-corrected to 11.03.2011) and the additional use of $^{135}Cs$ may also distinguish between different reactor units as in Fukushima Daiichi NPP.[35] Another example for the application of isotopic ratio analysis for nuclear forensics is the radioxenon isotopic ratio from emission of research reactors focusing on producing medical isotopes from high-enriched uranium (HEU) or LEU. The isotopic xenon ratios allow chronological assessment of the origin of the noble gas isotopes from underground nuclear weapons testing or civil production sources.[36] It is also possible to correlate radioisotopes with their respective stable isotopes due to the fact that in nuclear fission neutron rich isotopes are produced favorably, which changes the found isotopic ratio from the anthropogenically undisturbed isotopic ratio found in nature [37] or even to the sample's trace metal content. [38] The use of parent-daughter isotopic ratio [39] and isotope fingerprints allows also assignment to the origin of the radioactive material.

Generally, the focus for nuclear forensics lies on the analysis of actinides, major fission products $^{89+90}Sr$, $^{134+137}Cs$, $^{131}I$, noble gases and fissile nuclides $^{235}U$, $^{239}Pu$. However, minor radionuclides $^{22}Na$, $^{103,106}Ru$ have proven to be able to underpin evidence.[2, 40] Especially minor radionuclides can illuminate different aspects of a release process inside a reactor.

## 1.4 Summary

The field of nuclear forensics focuses on detecting of illicit trafficking, age dating of nuclear material, and identifying the source of nuclear material. The discipline of environmental nuclear forensics further concentrate on the origin of a radioactive contamination in the environment. It utilizes a combination of chronology, radiochemistry, isotopic ratio measurements, and radioecology to determine the sources of radioactive material released into the environment. In some cases, even mixtures of different contamination sources can be distinguished. This allows conclusions to be drawn about the origin of the source as well as possible release processes (timing and scenario). In order to make conclusive statements, these must be supported by several calculated and experimental data from all combined fields.[26]

# Chapter 2

# Nuclear forensics of noble metal radionuclides

## 2.1 Introduction

Noble metals belong to the transition elements. The metallic form of the noble metals exhibits a significant resistance against chemical attacks and can only be dissolved in one or a combination of strong acid solutions or complexing agents. The abundance of noble metals in the Earth's crust are the lowest of all element groups. The list of noble metals consists of the following elements: copper (Cu), ruthenium (Ru), rhodium (Rh), palladium (Pd), silver (Ag), rhenium (Re), osmium (Os), iridium (Ir), platinum (Pt), gold (Au), and mercury (Hg). Noble metals generally show a relatively high positive standard electrode potential.[41]

The noble metals can be further subcategorized into the platinum group elements (PGEs) containing Ru, Rh, Pd, Os, Ir, and Pt. The PGEs show similar physical and chemical properties and can be found in nature accompanied in mineral deposit.

## 2.2 (Radio-)silver

Silver is a transition metal element with an electron configuration of $[Kr]4d^{10}5s^1$. Due to the configuration with a singular electron filled in the s shell, metal silver has several distinct chemical properties. Metallic silver is a silvery white metal with ductile and malleable properties and has the highest electrical conductivity known in metals and high thermal conductivity. Silver can be found in the lithosphere with an abundance of 0.08 parts per million, mostly in the form of the solid metal or bound in sulfide minerals.[41, 42]

### 2.2.1 Chemistry

Silver belongs to the noble metals, for which reason silver can be reduced to its metallic form with heat or base metals. The oxidation state Ag(I) is the most stable, because of the electron configuration of silver. In aqueous solution only the oxidation state Ag(I) is stable. The oxidations states Ag(II) and Ag(III) are less common and merely found under strong oxidation conditions, in complexes and in form of solids.[43] The silver cation $Ag^+$ has several soluble counter anions e.g. nitrate $NO_3^-$, fluoride $F^-$, perchlorate $ClO_4^-$, bromate $BrO_3^-$, sulfate $SO_4^{2-}$, acetate $CH_3COO^-$, and tartrate $C_4H_4O_6^{2-}$. The cation also forms various precipitates with the insoluble counter anions such as the halogenides chloride $Cl^-$, bromide $Br^-$, iodide $I^-$, as well as hydroxide $OH^-$, sulfide $S^{2-}$, carbonate $CO_3^{2-}$, and oxalate $C_2O_4^{2-}$.

For the separation of radiosilver, several typical separation methods such as precipitation, chemical reduction, coprecipitation, complex forming, and ion exchange are employed. The precipitation of silver can be used in gravimetric analysis, as most precipitates are quantitative. Sundermann *et al.* reported several usages of chloride

precipitation for radiosilver determination as many interfering radionuclides are not co-precipitated.[43] For the chloride precipitation, an excess of chloride anions needs to be avoided due to forming of soluble chloride complexes $[AgCl_2]^-$, $[AgCl_3]^{2-}$ and $[AgCl_4]^{3-}$ (cf. Figure 7).[44, 45]
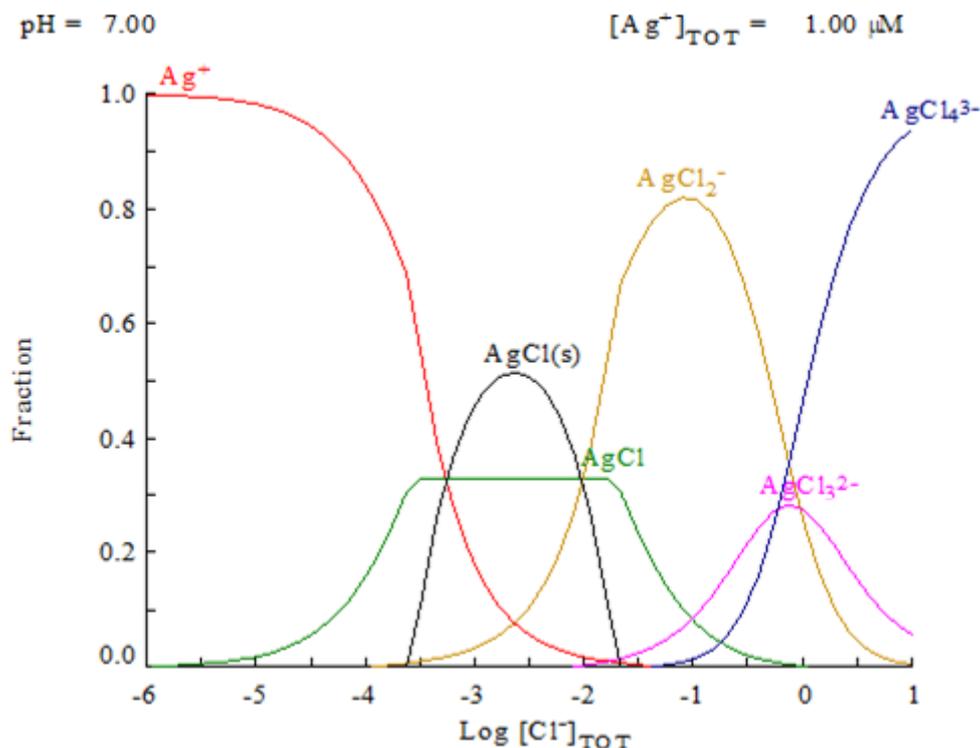


Figure 7: Fraction of silver species present in a silver chloride system at pH=7.00 with a silver concentration of $10^{-6}$ mol·L$^{-1}$.[45]

A silver chloride precipitate from a nuclear waste solution needs to be cleaned by complexation with dilute ammonia. The ammonia complex can thereafter be decomposed by volatilization of ammonia and precipitated for radiochemical purity of the silver precipitate. The purified silver precipitate from fission product solution can still have contaminations with antimony, iridium, ruthenium, and palladium. Another separation method is the chemical reduction and precipitation of the silver by addition of reducing agents such as formic acid, ferrous sulfate, stannous chloride, metallic zinc and ascorbic acid. Silver can also be separated by co-precipitation with iron hydroxide and tellurium. Furthermore, silver can form several inorganic and organic complexes such as the commonly known ammonia complex $Ag(NH_3)_2)^+$. Moreover, silver shows a high affinity to sulfur atoms, for which reason it forms complexes with dithiazone and diethyldithiocarbamate, which can be used for organic extraction. In addition, ion exchange can be used for separation of silver. Typical cation exchange resins DOWEX-50 and AG50W-X8 have shown good separation for the cation $Ag^+$ and anion exchange resin can be used for the anionic cyanide complex $Ag(CN)_2^-$. For low quantities of radiosilver and good decontamination, isotopic exchange can be employed in a silver nitrate solution with a silver chloride precipitate as the isotopic equilibrium is reached

30

fast and the contamination with other radionuclides are sparse. Furthermore, silver can be electrodeposited on platinum in a solution of sodium cyanide and sodium hydroxide with the advantage of a good separation from halogenides with focus on the separation from iodine.

During the gamma analysis of Fukushima food samples from the publication Weller *et al*. [46], noticeable activity concentrations of $^{108m}$Ag and $^{110m}$Ag were found in seafood. The low activity concentration of the radiosilver isotopes and the increased detection limits due to the strong presence of other interfering gamma emitters $^{134}$Cs and $^{137}$Cs hindered the analysis. For this reason, the publication **D1** focuses on the development of a robust and easy-adaptable method for the separation of radiosilver from other interfering gamma-emitters.[47] Autodeposition is a widely used method for the separation of radionuclides from solution, such as the separation of polonium isotope $^{210}$Po on a silver waver.[48] Due to the electrochemical properties of silver, we could prove in publication **D1** the suitability and efficiency also for the reduction of radiosilver in the presence of a copper plate in ammonia solution under the following reaction:[47]

$$2\ [Ag(NH_2)_2]^+ + Cu^0 \rightarrow 2\ Ag^0 + [Cu(NH_3)_4]^{2+} \quad \Delta E_0 = +0.696\ V$$
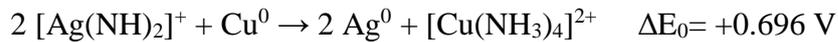
Generally, most silver compounds can be dissolved in nitric acid. In presence of palladium, the dissolution process in nitric acid is slowed down and the use of aqua regia is favored. In case, that the silver compound is not dissolvable with nitric acid, complexing agents such as ammonia and cyanide can be used. Organic material can be ashed and dissolved in nitric acid or wet digested.[43]

Schweitzer *et al*. reported the possibility of silver forming radiocolloids. Radiocolloids are agglomerates of radionuclides in low concentration solutions ($\leq 10^{-8}$ mol/l). A solution of $^{111}$Ag without silver carrier was tested for the removal of silver by centrifugation and filtration.[49] A coagulation time of around 30 min for silver with high pH dependency was reported. The centrifugation technique removed more colloids than filtration, for which reason the colloid forming by adsorption was refuted. [49] In contrast, Hamester *et al*. suggested the production of silver radiocolloids by adsorption of siliceous and organic dust.[50]

### 2.2.2 Isotopes

Silver has two stable isotopes $^{107}$Ag (51.84 %) and $^{109}$Ag (48.16 %) with almost equal abundances. In iron meteorites the $^{107}$Ag/$^{109}$Ag isotopic ratio is found to enhanced with up to 212% from the terrestrial value due to subsequent decay of cosmic $^{107}$Pd.[51] Several radioisotopes of silver are known from $^{93}$Ag to $^{132}$Ag. Various silver radioisotopes have nuclear isomers. Nuclear isomers are metastable "m" isotopes, which have an excited nucleus with a half-life longer than $10^{-9}$ s. The half-life of some silver nuclear isomers exceed the half-life of the ground states e.g. $^{108m}$Ag ($T_{1/2}$=437.7 a); $^{108}$Ag ($T_{1/2}$=2.38 min) and $^{110m}$Ag ($T_{1/2}$=249.8 d); $^{110}$Ag ($T_{1/2}$=24.6 s). This occurs, when the decay is delayed to the ground state due to a forbidden transition such as a nuclear spin

change.[52] A section of the nuclide chart of selected radioisotopes are presented in Figure 8.

Both metastable radionuclides of silver [108m]Ag and [110m]Ag have several gamma emissions to count, for which reason the quantification via gamma spectrometry is preferred. Due to cascade emitting of gammas from different nucleus energy levels, the gamma emissions are prone to forming of coincidence summations peaks, which need to be taken into account.
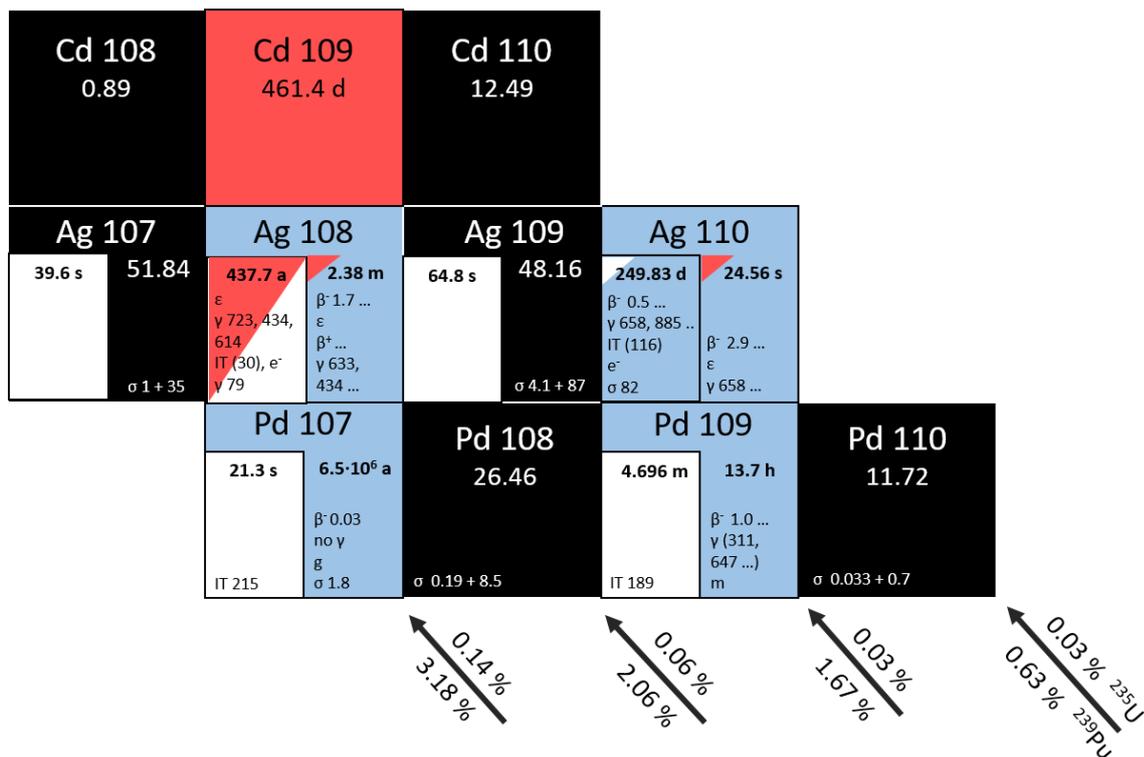


Figure 8: Detail of the nuclide chart. Data taken from Magill *et al.* [53]

### 2.2.3 Industrial and nuclear application

In most PWR, the control rods consist out of an Ag-In-Cd (80 % silver, 15 % indium and 5 % cadmium (SIC)) alloy. The control rod is build similar to fuel rods with a zirconium alloy guide tube and stainless steel cladding filled with the alloy and helium filler gas. Petti calculated that a core of a 3000 MW thermal PWR holds up to 2800 kg of the Ag-In-Cd alloy, which is initially 2 % of the core mass.[54] Dubourg *et al.* investigated a hypothetical scenario of SIC control rod failure during a severe accident.[55] The alloy has a relatively low melting point of 800-850 °C in comparison to the other core components.[54] The molten SIC alloy will initially be retained in the stainless steel cladding, and with rising temperatures different rod failure can occur. A failure of the steel cladding can be observed at temperature exceeding 1200 °C, which leads to deforming of the control rods and releasing the melt, and downward migration. Furthermore, aerosol of indium and cadmium, and to a lesser degree silver will be released in the reactor core. Cadmium is the most volatile of the SIC alloys and will have

a high vapor pressure. Silver is mostly vaporized as monoatomic $Ag_{(g)}$ and minor species $Ag_{2(g)}$ and $Ag_2O_{(g)}$. The released indium and silver can react with the iodine fission products, enabling different transportation ways in the core.[54, 55]

The PWR Three Miles Island Unit 2 (TMI-2), which had a partial core melt down in 1979 after three months of operation, had used SIC as control rod material with a masses of 2200 kg silver, 412 kg indium, 137 kg cadmium.[17] Studies from Akers *et al.* have shown that the SIC alloy melted during the TMI-2 accident, and proved failure of the control rods. Parts of the SIC volatilized and were found in the core upper part, but most relocated downwards, which probably led to dissolution of parts of the zirconium alloy cladding of the surrounding fuel rods. A large part of SIC alloy inventory remained during the accident in the core region and the reactor pressure vessel, and less than 1% was released into the environment.[17] With data taken from Lepel *et al.* on the activation of the SIC control rods,[56] we calculated in the publication **D1** the silver isotopic ratio of $^{108m}Ag/^{110m}Ag$ in spent control rods higher than 10.[47] Due to the short operation time of 3 months of TMI-2, the neutron activation products and isotopic ratio of the radiosilver isotopes is probably lower, unfortunately, neither measured nor calculated data on radiosilver activities or isotopic ratios from the TMI-2 accident are available for comparison.

Hirschberg *et al.* described sources of radiosilver $^{110m}Ag$ from radioactive corrosion products in the primary cooling circuit of VVER-type PWRs.[34] Corrosion products are dissolved compounds from construction materials such as welding materials, which are transported and activated in the core. The activated corrosion products can thereafter be deposited on the surfaces of the primary circuit. At pH=7 following the Pourbaix diagram, the present silver species consist mostly of $Ag^+$ species and $Ag_2O$ in dissolved and colloid form. The cation $Ag^+$ is stable in neutral and slightly alkaline solution with only moderate hydrolysis. In lower potential regions mainly $Ag^+$ is found and $Ag_2O_3$ is found in high potential areas. The dominating silver species are adsorbed on austenitic stainless steel, involving a slow surface transformation and continuous build-up of a passive oxide layer. In this passive oxide layer, the silver ions are reduced and forms an adherent contamination.[34]

Furthermore, in LWR the reactor pressure vessel is generally sealed with base tubing of metallic head seals consisting of pure silver. Due to the closeness to the core center, neutron flux density reaches up to $10^7$ cm$^{-2}\cdot$s$^{-1}$ in LWR at the reactor pressure vessel head. This source may be the reason for the detection of $^{110m}Ag$ in the Fukushima environment.[46] LWR are generally operated for 35-40 years, which lead to high activities of neutron activation products. Silver is also often employed in reactor cores as beta-emission neutron detectors, which allow direct measurement of neutron flux energy distribution in the core.[57, 58] Moreover, the reactor core holds other potential sources of stable silver. Fresh nuclear fuel contains impurities of several elements such as up to 5 g silver per ton heavy metal.[33] And after irradiation und build up fission products and

activation products, ε particles and metallic precipitates of Mo, Ru, Os, Tc and Rh/Ag are found in nuclear fuel.[32]

### 2.2.4 Environmental behavior

When considering the environment, the transport of silver plays its major role in the hydrosphere. Yamazaki *et al*. reported the accumulation of silver in fish. The main fraction of silver is hereby accumulated in the fish liver.[59] It is highly possible that small amounts of silver (such as given by releases of radioactive silver isotopes) form chloride complexes in seawater medium. The chloride concentration in seawater is generally around 0.5 mol·L$^{-1}$, which indicates a predominant soluble $[AgCl_4]^{3-}$ species from the speciation diagram in Figure 7. During operation of early NPPs, waste water effluents were often released directly into the nearest aquatic system and e.g. annual releases of 37 MBq of $^{110m}$Ag from Humbold Bay NPP (US) was reported in 1971-1972. The effluents of radiosilver into seawater are relatively homogenous dispersed, which favors the possibility of the existence of radiosilver complexes over the occurrence of particulate matter. In contrast, in river water at pH=8 and 10 µg·kg$^{-1}$ silver is reported to generally form 50 % of particulate matter, which precipitates. For this reason, 80 % of the silver content is adsorbed rapidly in freshwater, and desorbed in seawater media. The pH of the aquatic media only has moderate influence on the silver adsorption/desorption equilibria.[60] Beasley *et al*. found both metastable isotopes $^{108m}$Ag and $^{110m}$Ag in the upper layer of the ocean from atmospheric nuclear weapons testing at Bikini Atoll. The silver isotopes accumulated primarily in mussels and oysters, which can be used as bioindicators.[61] Folsom *et al*. proposed, that the isotopic ratio $^{108m}$Ag/$^{110m}$Ag from weapons fallout can be used for time correlation of nuclear detonations, due to the primarily production pathway by neutron activation of silver in nuclear weapons. Furthermore, radiosilver was found after the Fukushima Daiichi NPP accident in 2011 in oyster, abalone,[46] as well as wharf roaches.[62] It is also known, that the dissolving mechanism in freshwater of engineered Ag nanoparticles as well as natural colloids is strongly dependent on the presence of dissolved organic matter (DOM).[63]

The radiosilver isotopes were also present in the dry and wet deposits from the nuclear accidents of Chernobyl NPP and Fukushima Daiichi NPP. Pfau *et al*. reported in 1986 after the deposition of Chernobyl fallout an isotopic ratio of $^{110m}$Ag/$^{137}$Cs=0.02 in hay. The deposited silver is then found to be bioaccumulated in sheep liver with up to $^{110m}$Ag/$^{137}$Cs=1.7.[64] The Chernobyl fallout radiosilver was also present in opencast silver mines in Serbia with an activity concentration reaching up to 1250 Bq·kg$^{-1}$.[65] The calculated inventory of $^{110m}$Ag was calculated to $6.2 \cdot 10^{15}$ Bq [64] and $2.1 \cdot 10^{15}$ Bq [66], respectively. The activity is calculated to around 18 kg of natural silver, which is consistent with the amount of in-core silver neutron detectors and neutron activation of natural silver. After the Fukushima Daiichi NPP accident, radiosilver was determined on concrete surface of the reactor buildings. Radiosilver activity concentration were around 1/10 of the $^{137}$Cs activity concentration and mostly present as dust particles and structural

fragments produced by hydrogen explosions in Unit 1 and 3, whereas Unit 2 exhibited lower radiosilver activities in form of adherent contaminations.[67] The radiosilver isotope $^{110m}$Ag was also found in soil in coastal areas around the NPP. The activity ratio $^{110m}$Ag/$^{137}$Cs varied from 0.002 to 0.008 with activity concentration ranging from 2 to 2,400 Bq·kg$^{-1}$ in coastal soil. Radiosilver was mostly retained in the upper layer of the 0 - 20 mm sediment soil due to sorption on clay and silt fraction.[68] After deposition in soil, silver is expected to immobilize fast as insoluble silver chloride precipitates. Experiments of Szabó *et al*. with the soft base chelating agents diethyldithiocarbamic acid and tetrathiacyclohexadecane-3-11-diol have shown that not all silver is completely immobilized. For this reason, silver seems to be mobilized in presence of humic substance, attributing to the uptake in organism. Natural organic compounds and hydrous oxides of iron and manganese serve as adsorptive phases for trace metals such as silver. Conclusively, correlation with binding of silver to soil organic matter is reported.[69] Publication **D1** focused on the fate of freshly deposited radiosilver contamination in soil.[47] The study showed a strong binding of silver to the residual fraction after several chemical extraction steps and thus indicating a rather low mobility. As mentioned above, the presence of natural organic compounds can significantly increase the mobility of silver in soil and thus the potential uptake by organisms. For this reason, the bioavailability of silver was investigated in publication **D2**.[70] A typical Japanese eadible mushroom species *Lenitula edodes* (Shiitake mushroom) was chosen as the reference organism. One reason was that mushrooms are prone to accumulation of various elements (alkaline metal [71], heavy metals [72, 73]). Another reason was that the Shiitake mushrooms were grown on sawdust substrate, which resulted in high content of organic matter, possibly affecting the uptake of silver. No bioaccumulation of silver was found in Shiitake mushrooms when tested by various analytical methods

## 2.3 (Radio-)palladium

Palladium belongs to the PGEs in the transition series of ruthenium, rhodium, and palladium with an electron configuration of [Kr]4d$^{10}$. Comparable with the physico-chemical properties of platinum, palladium displays a similar white metallic appearance and the mechanical properties of a soft and ductile metal. It has the lowest melting points of the PGEs. Palladium is generally found as in alloys with gold in nickel-copper deposits or platinum metal deposits with an overall abundance of 0.01 parts per million in the earth's crust.[41, 42]

### 2.3.1 Chemistry

The pure metal palladium is relatively inert. Palladium shows no reaction with oxygen at room temperature. The first observable reaction with oxygen starts at 800 °C, which builds-up a palladium oxide PdO layer. Palladium compounds are generally in the oxidation state of 0 and +II, with lesser abundances in +IV and +III. Metallic palladium is only be slightly attacked by conc. HCl, but rapidly dissolved in conc. HNO$_3$ and aqua

regia, Due to its electrochemical nobility, palladium can be precipitated as a metal by several reagents. Palladium dichloride solution e.g. is reduced to the metal by hydrazine hydrate, potassium nitrite, phosphorus, formic acid, methane, and ethylene. Ethylene can be used for separation from other PGEs. Palladium can form stable complexes in solution, which are not easily reducible. The reduced metal can be in form of a colloidal metal or palladium sponge and palladium black. When palladium is oxidized in solution, the black monoxide PdO forms. Under suitable conditions the instable dioxide compound $PdO_2$ is formed, which precipitated as dark red hydrate and subsequently decomposes to the monoxide. The anhydrous palladium dichloride has red hydroscopic crystals, which are easily soluble in water as $PdCl_2 \cdot 2\ H_2O$ and in HCl while forming chloride complexes. Palladium can also form anion and cation complexes. In the presence of significant amounts of chloride ($>10^{-4}\ mol \cdot L^{-1}$), palladium forms various chloro-complexes $PdCl^{+}$, $[PdCl_3]^{-}$ and $[PdCl_4]^{2-}$. The degree of complexation increases with the amount of chloride present.[74] In sea water ($\sim 0.5\ mol \cdot L^{-1}\ Cl^-$) or other saline solution, the tetrachloropalladite species is predominant under oxidizing conditions (s. Figure 9 $E_h$-pH diagram). The chloride species are a major factor in the Pd transport in the aquatic environment.[75] The possible mobilization of palladium via chloride species needs to be taken into account by seawater releases or releases in deep geological repositories on basis of salt during water leakages scenarios.
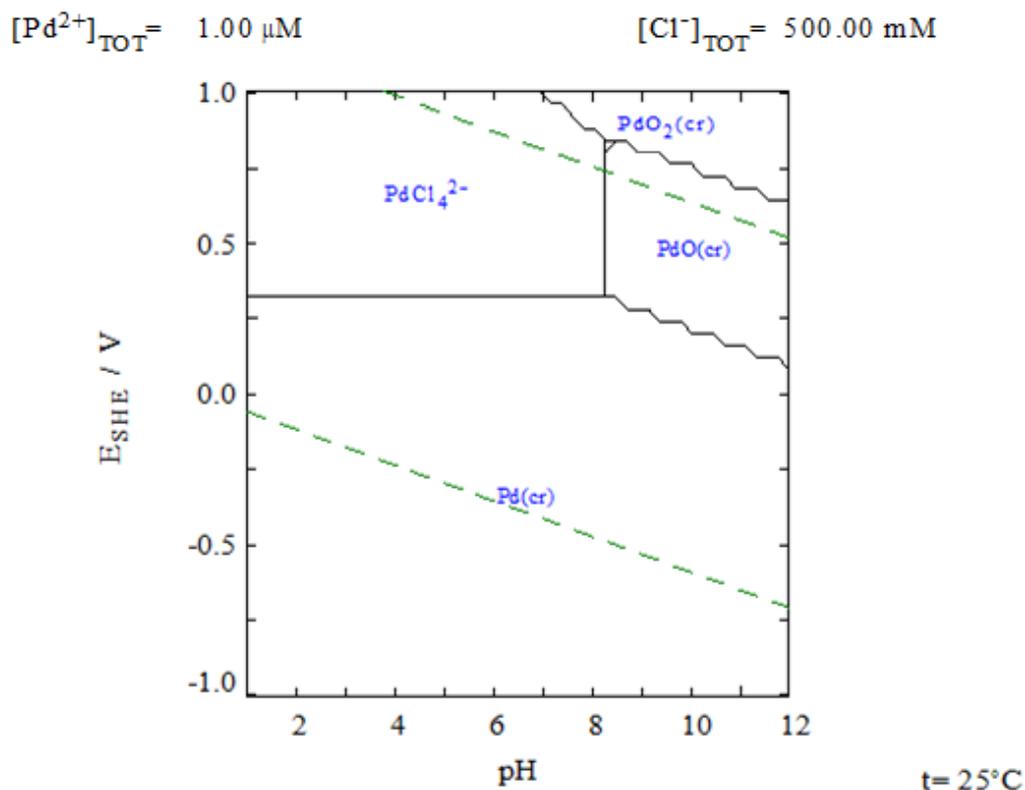


Figure 9: $E_h$-pH diagram of $10^{-6}\ mol \cdot L^{-1}\ Pd^{2+}$ and $0.5\ mol \cdot L^{-1}\ Cl^-$ system. The black lines indicate the transition area of the palladium species. The dotted lines are the stability boundaries of water. [45]

Further anion complexes are formed with $CN^-$, $CNS^-$, $NO_2^-$, $Br^-$, and $I^-$. A typical cation complex is the tetra amine complex $[Pd(NH_3)_4]^{2+}$. Furthermore, palladium forms

several chelate complexes with bindings to nitrogen, oxygen and sulfur atoms. The most famous palladium chelate complex is the dimethylglyoxime complex. The chemical structure of the palladium dimethylglyoxime complex is shown in Figure 10. The bindings of palladium with carbon atoms have been known for a long time and are commonly used in catalysis of various organometallic reactions utilizing the interconversion of Pd(II) to Pd(0) (e.g. vinylations, hydrogenation, carbonylation, oxidative coupling, cross-coupling, arylation and hydrogen shift reactions).[76–78]
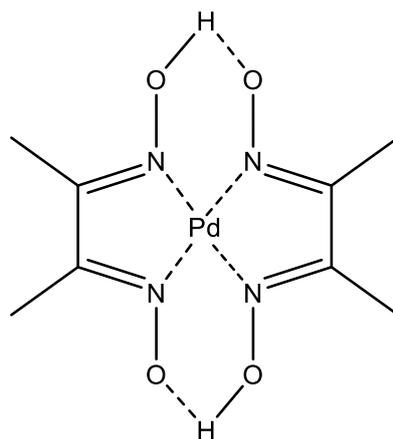


Figure 10: Chemical structure of palladium dimethylglyoxime complex.

For the separation of palladium, typical analytical separation methods as precipitation, solvent extraction, ion exchange and electrodeposition are employed. Palladium can be concentrated from dilute solution with coprecipitation with e.g. elemental tellurium. For this co-precipitation, tellurite is reduced with stannous chloride or other strong reducing agents. The co-precipitation is accompanied by gold, silver, and rhodium. After the precipitation, the tellurium can be removed by volatilization with ignition. Furthermore, palladium can be precipitated with hydrogen sulfide in the presence of lead ions. For the separation of other platinum metals, gold and basic metals, palladium can be precipitated with cyanide or iodide. However, silver, copper, and lead are co-precipitated. Moreover, palladium is specifically precipitated by reduction with ethylene. For precipitation of palladium, mostly dimethlygloxime is used. Palladium is precipitated by dimethylglyoxime in dilute acid solution, which is marginally soluble in water, dilute nitric or hydrochloric acid. The precipitate is readily soluble in ammonia, chloroform, and benzene. The precipitate can be decomposed by addition of conc. nitric acid and aqua regia. A common solvent extraction method also employs the formation of the Pd dimethylglyoxime complex with extraction into an organic chloroform phase. Furthermore, palladium can be retained on a cation exchange resin e.g. DOWEX-50. The cation exchange resin is loaded with diluted perchloric acid solution of palladium without an excess of halogenides. The retained palladium can then be quantitatively eluted with dilute hydrochloric acid. Palladium compounds can be dissolved in aqua regia, nitric acid, and sulfuric acid.[74]

### 2.3.2 Isotopes

Palladium has six stable isotopes: $^{102}$Pd (1.02 %), $^{104}$Pd (11.14 %), $^{105}$Pd (22.33%), $^{106}$Pd (27.33 %). $^{108}$Pd (26.46 %) and $^{110}$Pd (11.72 %). In addition, Palladium has several radioisotopes with characterized isotopes ranging from $^{91}$Pd to $^{129}$Pd. The radioisotope $^{107}$Pd has the longest half-life of the palladium isotopes with a half-life of 6.5 million years and decays to stable silver isotope $^{107}$Ag (cf. Figure 8). The existence of radiogenic $^{107}$Pd can also be linked to iron meteorites to a nucleosynthetic event in the solar system.

The long-lived $^{107}$Pd isotope is a pure beta emitter with a low beta endpoint energy of 34 keV. Due to the long half-life and only emission of beta radiation with low energy, the determination of $^{107}$Pd with radiometric methods allows only the detection of isolated $^{107}$Pd and/or high amounts of the radionuclide. There have been several attempts for the separation and determination of $^{107}$Pd in HLW, but most HLW samples did not exceed the detection limits ranging from 0.002 to 13,000 µg·kg$^{-1}$. The first report of $^{107}$Pd determination was published by Asai *et al.*, who measured 239 ng $^{107}$Pd per mg $^{238}$U in spent nuclear fuel.[79] For the separation and concentration of $^{107}$Pd, different methods were proposed: Anion exchange resin of the chloro-complex[80], Ni Resin with active compound dimethylglyoxime[81], coprecipitation of Pd as AgCl and Fe(OH)$_3$ with subsequent precipitation with dimethlyglyoxime[82], and laser induced photoreduction.[79, 83] For radiometric analysis, LSC measurements with direct DPM count [81] or TDCR mode [82] were employed. As an alternative, ICP-MS measurements are proposed with a dynamic reaction cell (DRC) [80] or reported with a single ICP-MS[79] and ETV-ICP-MS.[84] Asai *et al.* proposed the application of HR-ICP-MS or MC-ICP-MS for a better separation of isobars, however, with higher resolution, higher detection limits need to be taken into account. To date, according to the best of my knowledge, no $^{107}$Pd was determined in environmental samples. The paper **D3** was the first research paper with a mass spectrometric approach with a collision and reaction cell for a $^{107}$Pd determination in environmental samples from the Chernobyl exclusion zone. [85] The combination of a pre-separation and -concentration of minute-amounts of palladium on cation-exchange resins and Ni Resin$^©$ and subsequent measurement of the $C_2H_4$-mass-shifted palladium allowed a clean separation of $^{107}$Pd from isobaric and polyatomic interferences such as $^{107}$Ag$^+$ and $^{91}$ZrO$^+$. This enables the detection of environmental activities of $^{107}$Pd in the mBq·kg$^{-1}$ range.

### 2.3.3 Industrial and nuclear application

Palladium resources have major application in catalysis, electronics, and technology with a growing market for hydrogen storage. As already mentioned in Chapter 2.3.1 on the chemistry of palladium, palladium shows a high affinity towards carbon, nitrogen, hydrogen, and oxygen atoms. For this reason, Pd(II) compounds are key components for several organometallic reaction. Palladium serves in these reactions as heterogeneous catalyst. Palladium(II) chloride catalyzes the oxidation of carbon monoxide and can therefore be used in carbon monoxide detectors. Palladium can also be found as vehicle

exhaust catalysts to reduce the emission of carbon monoxide and nitrogen oxides by catalyzing their oxidation. Furthermore, palladium is widely used in electronics, as e.g. palladium-silver alloy electrodes in multilayer ceramic capacitors. Moreover, Pd serves as soldering and plating material. Based on the versatile interactions of palladium with hydrogen, several applications can be derived. The storage of elemental hydrogen in palladium at room temperature is currently often discussed, owing to the reason of the readily adsorption of hydrogen on palladium under the formation of palladium hydride. The hydride shows exceptional good ductility enabling a safe storage, however, the feasibility is rejected due to the high market price of palladium. Heated palladium membranes can also be used for the production of high-purity hydrogen due to its good hydrogen diffusion ability. [86]

Palladium or its compounds are not utilized in nuclear reactors for construction or nuclear materials. Nevertheless, palladium is continuously produced throughout the NPP operations by nuclear fission with a significant thermal neutron fission yield for $^{235}$U and $^{239}$Pu (FY) (cf. Table 2). The neutron-poor palladium isotopes $^{102}$Pd and $^{103}$Pd are not produced by fission of $^{235}$U or $^{239}$Pu from the respective isobar 102 and 103 due to shielding from the stable $^{102}$Ru and $^{103}$Rh isotopes. The fission yield of $^{104}$Pd is almost negligible because of the stable $^{104}$Ru isotope of the respective isobar and low direct fission yield of $^{104}$Rh and $^{104}$Pd. In contrast, all non-shielded neutron rich isotopes $^{105}$Pd to $^{112}$Pd show significant chain fission yields for both $^{235}$U and $^{239}$Pu.

Due to rising palladium prices, several patents and research papers have proposed the recovery of palladium from nuclear spent fuel, as it contains up to 0.1% palladium. [87, 88] In these proposals, the long-lived $^{107}$Pd would also be recovered, making the Pd fraction slightly radioactive, which should be taken into consideration for its application and before implementation into the Pd cycle.

Table 2: Summarized properties of selected palladium isotopes. For simplification, only the half-life of the ground state nuclide is shown.[53]

| Nuclide | Stable (Abundance), radioactive ($T_{1/2}$) | Thermal neutron fission yield of $^{235}$U in % | Thermal neutron fission yield of $^{239}$Pu in % |
|---|---|---|---|
| $^{102}$Pd | Stable (1.02 %) | 0 | 0 |
| $^{103}$Pd | Radioactive (16.99 d) | 0 | 0 |
| $^{104}$Pd | Stable (11.14 %) | $1.5 \cdot 10^{-8}$ | $5 \cdot 10^{-6}$ |
| $^{105}$Pd | Stable (22.33 %) | 0.95 | 5.76 |
| $^{106}$Pd | Stable (27.33 %) | 0.41 | 4.19 |
| $^{107}$Pd | Radioactive ($6.5 \cdot 10^{6}$ a) | 0.14 | 3.18 |
| $^{108}$Pd | Stable (26.46 %) | 0.06 | 2.06 |
| $^{109}$Pd | Radioactive (13.7 h) | 0.03 | 1.67 |
| $^{110}$Pd | Stable (11.72 %) | 0.03 | 0.63 |
| $^{111}$Pd | Radioactive (23.4 min) | 0.02 | 0.31 |
| $^{112}$Pd | Radioactive (21.0 h) | 0.01 | 0.13 |

## 2.3.4 Environment

The mobility and solubility of palladium increases under suitable conditions depending on the formation of inorganic or organic complexes. The amount of dissolved palladium correlates with the pH, chloride content and total suspended solids in the aquatic environment. During wet deposition, palladium from atmosphere and road dust have shown to accumulate in water systems. Palladium and its inorganic and organic compounds have a higher bioavailability than the respective compounds of other PGEs.[89, 90] Small organic acids such as oxalates and acetates form complexes with Pd, which can influence the Pd solubility of soil solution.[91] Furthermore, palladium is known to form soluble bioaccessible species of Pd in presence of anionic several species such as $Cl^-$, $NO_3^-$, $SO_4^{2-}$, $PO_4^{3-}$.[92] Only scare studies have been published on the bioavailability of palladium in plants and fauna as well as terrestrial and aquatic animals. [93, 94] Due to the general low concentration of palladium present in the environment, mainly in direct consequence of civilization, the toxicity of palladium to the environment and human is presumed low. Some in vitro studies have shown the potential to inhibit cellular functions due to the formation of complexes. Also sensitization of PGEs and its compounds have been noticed.[95] However, due to the rising palladium concentrations in the environment, a possible toxicological impact needs to be further investigated.[86]

To the best of my knowledge, there have been no reports on the existence of radiopalladium in the environment yet, until our recent potential discovery of $^{107}$Pd in Chernobyl NPP cooling pond sediment (**D3**).[85] The short-lived $^{109}$Pd and $^{112}$Pd are

40

listed by the National Radiation Laboratory to be likely visible during the first 10 days of airborne radioactive releases in the CTBT monitoring stations.[96]

## 2.4 Isolation and extraction of noble metal radionuclides

As previously described in Chapters 2.2.1 and 2.3.1, isolation and extraction of noble metal radionuclides can be performed with various methods such as (co-)precipitation, extraction chromatography, complexation, electro- and autodeposition and isotopic exchange. However, not all methods are feasible for ultra-trace analysis to achieve sufficient purity from interfering nuclides, while at the same time having sufficient chemical yield. This is the case for the precipitation of silver in low quantities in publication **D1**.[47] A sole precipitation for isolation of radiosilver have been proven disadvantageous as the interfering radionuclide $^{137}$Cs could not be completely eliminated. Generally, low quantities of radionuclides are often interfered by dominating other radionuclides in radiometric methods or by isobaric interferences in mass spectrometry from other stable or radioactive isotopes and compounds. For a proper measurement, the interferences need to be eliminated or at least reduced. The interference reduction can often be performed by chemical means. The employed chemical extractions are outlined in the upcoming sections.

### 2.4.1 Electrochemistry

Noble metal elements have a high positive standard potential. In Table 3, the standard electrode potential $E_0$ of aqueous solution under standard conditions is presented. The order and potential can change in different types of media and conditions. Cu has the lowest and Au the highest standard electrode potential of the noble metals. [42, 97]

The separation techniques of electro- and autodeposition utilizes the electrochemical potential of a solution. The electrodeposition or electroplating is a process of the reduction of a metal ion to a surface (electrode) by applying an electric potential and current. In contrast, the autodeposition describes the process of a spontaneous deposition of the analyte on the surface by simple reduction-oxidation (redox) reaction in the presence of an element of lower electrochemical potential. Due to the high difference in electrode potential of Cu and Ag, the redox reaction with autodeposition of silver ions onto elemental Cu occurs naturally.[98, 99] Under consideration of several aspects such as kinetic inhibition, adhesion and complexing agents, Ag and other elements with higher electrode potential than Cu can be selectively deposited and later measured. The separation of traces of radiosilver by autodeposition was investigated in **D1**.[47]

Table 3: Standard electrode potential $E^0$ in V of noble metal ions in water.[42, 97]

| Nobility | Element | oxidant $\rightleftharpoons$ reductant | $E^0$ [V] |
|---|---|---|---|
| | H | $2\ H^+_{(aq)} + 2\ e^- \rightleftharpoons H_{2(g)}$ | 0.00 |
| | Cu | $Cu^{2+}_{(aq)} + 2\ e^- \rightleftharpoons Cu_{(s)}$ | 0.34 |
| | O | $O_{2(g)} + 2\ H_2O_{(l)} + 4\ e^- \rightleftharpoons 4\ OH^-_{(aq)}$ | 0.40 |
| | Re | $Re^{3+}_{(aq)} + 3\ e^- \rightleftharpoons Re_{(s)}$ | 0.50 |
| | Ru | $Ru^{3+}_{(aq)} + 3\ e^- \rightleftharpoons Ru_{(s)}$ | 0.60 |
| | Ag | $Ag^+_{(aq)} + e^- \rightleftharpoons Ag_{(s)}$ | 0.80 |
| | Rh | $Rh^{3+}_{(aq)} + 3\ e^- \rightleftharpoons Rh_{(s)}$ | 0.80 |
| | Hg | $Hg^{2+}_{(aq)} + 2\ e^- \rightleftharpoons Hg_{(l)}$ | 0.85 |
| | Os | $Os^{3+}_{(aq)} + 3\ e^- \rightleftharpoons Os_{(s)}$ | 0.90 |
| | Pd | $Pd^{2+}_{(aq)} + 2\ e^- \rightleftharpoons Pd_{(s)}$ | 0.92 |
| | Ir | $Ir^{3+}_{(aq)} + 3\ e^- \rightleftharpoons Ir_{(s)}$ | 1.16 |
| | Pt | $Pt^{2+}_{(aq)} + 2\ e^- \rightleftharpoons Pt_{(s)}$ | 1.2 |
| | Au | $Au^{3+}_{(aq)} + 3\ e^- \rightleftharpoons Au_{(s)}$ | 1.5 |

## 2.4.2 Ion exchange and extraction chromatography

Liquid ion exchange and extraction chromatography currently presents the state of art in technology and science for separation and pre-concentration methods for several radionuclides.[100, 101]. The advantage of extraction chromatography lies in its simplicity and possibility to reduce time consuming sample preparations, as well as its sensitivity and resulting high purity of analyte fraction. In column extraction chromatography, the stationary phase consists of an organic extractant, which is embedded on an inert – often a polymeric – bed. The mobile phase is generally an aqueous solution.[102] Commonly, commercially available extraction chromatography resins often follow resembling analytical protocols:

1. Preconditioning with aqueous solution of the same matrix used for the sample solution.
2. Feeding of the sample solution to the column, hereby the analyte binds specifically to the stationary phase.
3. Washing with a similar or slightly modified washing solution to remove interfering matrix components and other radionuclides.
4. Finally, the analyte is eluted from the stationary phase by changing of the aqueous solution, e.g. varying the acidic strength, and collected individually. Ideally, the eluate has the needed matrix consistency for the followed-up analytical methods.

There are many resins with very specific properties for several analytes available. The CL Resin by Triskem International has an organic extractant, which is selective for

several PGEs, Au and Ag, but is not mentioned by name. The CL Resin was developed for the separation of chloride and iodide at a resin saturated with silver. Silver(I) shows a high weight distribution ratio of 65,000 mL·g$^{-1}$ in 1 mol·L$^{-1}$ H$_2$SO$_4$.[103] Due to the strong binding of silver, the retained silver can only be eluted by forming strong silver compounds such as with sodium sulfide. We tested the application for small quantities of $^{108m}$Ag with different agents and discussed the application in **D1**. Furthermore, TBP Resins by Triskem International was tested for radiosilver separation as the TBP Resin also exhibits good weight distribution ratios for silver (> 100 in 0.1 mol·L$^{-1}$ HCl).[104] The separation quality and chemical yield in different acid solutions were not satisfactory (**D1**).[47]

The Nickel Resin from Eichrom Technology Inc was developed for the separation of the neutron activated radionickel isotopes $^{59}$Ni and $^{63}$Ni in radioactive waste solution. The active organic extractant dimethylglyoxime (DMG) is coated onto an inert chromatographic bed. Ni is precipitated as red Ni(DMG)$_2$ at the column at pH=8-9 and washed with ammonium citrate. The precipitate Ni(DMG)$_2$ is eluted by dissolution of the complex in 3 mol·L$^{-1}$ HNO$_3$.[105, 106] It is long known, that palladium shows a similar affinity for DMG under precipitating as an orange Pd(DMG)$_2$ complex (refer to Chapter 2.3.1). In contrast to the Ni(DMG)$_2$ complex in slight alkaline media, the optimal precipitation of Pd(DMG)$_2$ is achieved in acidic media (pH=1-2). Dulanská *et al.* have already shown the feasibility of Nickel Resin for the separation of Pd from evaporated and concentrated samples after addition of stable Pd carrier.[81] For mass spectrometry methods, the addition of stable carrier is disadvantageous for the measurement. We proved in **D3** that the Pd chemical yield of Ni Resin is also suitable for low concentration of palladium present (10 µg and 10 ng Pd). [85]

## 2.5 Measurement techniques

### 2.5.1 Radiometric methods

Radiometric methods combine all methods for the detection of ionizing radiation for the determination and/or quantification of radionuclides. Typical radiometric methods are α-, β-, and γ-spectrometry. In general, α- and β-spectrometry are performed by Si-semiconductor detectors, limited with gas-filled proportional counters or liquid scintillation counting. In contrast, γ-spectrometry is predominantly measured via semiconductor or solid scintillation detectors.[107] In the following sections, the used methods γ-spectrometry via semiconductor detectors and imaging via autoradiography are briefly described.

The use of gamma spectrometry for γ radiation measurements is versatile yet straightforward. Gamma radiation is emitted during the relaxation of an excited nucleus after a preceding radioactive decay. However, not all decays result in an excited nucleus state, for which reason, not all radionuclides are γ emitters. Due to the energetically defined excitation states of a nucleus, the emitted γ energies are discrete and specific for

each γ emitter. A γ emitting radionuclide can have one or several excited states, which is often why more than one γ energy peak can be identified in a γ spectra of one radionuclide. Not all excited states are populated the same after the preceding decay, for this reason, each γ emission has its own emission probability. For the γ measurements in our laboratory, measurements were performed with semiconductor detectors of high-purity germanium (HPGe). The use HPGe detectors allow γ measurements with high sensitivity and excellent energy resolution of up to 0.5 keV at energies of several 100 keV. The high density of the semiconductor material increases the probability of interaction with γ rays and therefore its sensitivity. HPGe detectors are cooled by liquid nitrogen to avoid thermal excitation (noise) in the semiconductor with energy band gaps of around 1 eV. The γ rays produce an electron-hole pair by interaction with the semiconductor material's intrinsic region, which is collected at the electrodes within µs. The amount of electron-hole pairs is proportional to the absorbed energies of the γ rays. In a typical γ spectra various contribution from X- and γ rays are visible. While depositing the whole energy of a γ ray, a narrow photopeak with distinct energy is observed. Each photopeak is accompanied by a Compton continuum. The Compton continuum results from the Compton Effect, which describes the effect of the angle dependent scattering of a photon by interaction with an electron. The photon scattering can result in energy loss, which is dependent on the scattering angle. If the photon exhibits an energy higher than double the rest mass of an electron with 1022 keV, another effect is visible in the respective γ spectra: the pair production. Pair production describes the effect of the conversion of a photon to an electron-positron pair in the electromagnetic field of a nucleus. The opposite process is called electron-positron annihilation. The produced positron during the pair production is generally annihilated within the detector volume, which instantly produces two 511 keV photons and can be seen in the spectra as the annihilation peak at the respective 511 keV. Due to the limited detector volume, one or both of the produced 511 keV photons can escape the detection, which produces escape peaks of the residual photoeffect peak of the energy $E_p$ (single escape: $E_p$-511keV and double escape: $E_p$-1022 keV). Furthermore, some radionuclides show cascade emission of γ and X-ray photons. The cascade emission in extremely low time interval can lead to the detection of the sum of energies, resulting in sum peaks.[107] The counting statistics for photopeaks is dependent on the background of the spectra. For this reason, the Compton Continuum of dominant γ-emitter can significantly increase the detection limits of photopeaks of lower energies. This hinders or even makes the analysis of minute amounts of minor radionuclides in the diverse radioactive sample impossible. **D1** has a detailed calculation of detection limits for low quantities of [108m]Ag in presence of one dominant radioisotope [137]Cs.[47]

The autoradiography uses the exposure of photographic emulsion on plates with ionizing radiation from α or β radiation. The concept is closely related to the exposure of the photographic emulsion with visible light in analog photography. The autoradiography enables the localization the α or β emitters within a sample. Due to dependence of the resolution from the depth profile of a sample, only smooth and uniform samples can be

44

used to achieve a good resolution on the photographic film. The resulting radiograph is strongly dependent on the used photographic film, the sample material and format, the ionizing radiation and energy, the exposure time and the development of the radiographic film. For this reason, quantification of activities is complicated and only possible if all parameters are optimized and only one radionuclide is present. However, the localization and the strength of the exposure gives important qualitative information on the distribution and intensity of the radionuclides in the sample.[107] In this thesis, autoradiography was used for the localization and information on the bioavailability of $^{137}$Cs in Shiitake mushroom fruit bodies (**D2**).[70]

2.5.2 Mass spectrometric methods

Mass spectrometry (MS) is an analytical method, which uses the separation and analysis of different mass-to-charge ratio of ions. Inorganic MS usually is employed for the measurement of stable isotopes of different elements for ultra-trace analysis; however, the use for the measurement of long-lived radionuclides is continuously increasing. [108–111] A mass spectrometer generally consists of an ion source, a mass analyzer, and a detector. The principle of the used inductively coupled plasma quadrupole mass spectrometry (ICP-QMS) for the analysis of stable and long-lived noble metal isotopes is briefly discussed in the following section. In addition, the extra equipment as a triple quadrupole MS in combination with a laser ablation (LA) introduction system is explained.

The ICP-MS instrument is used for elemental and inorganic isotope ratio analysis. The ICP-MS is equipped with an inductively coupled plasma (ICP) as an ion source. The ICP ion source creates an Ar plasma through inductively heating of the Ar gas with an electromagnetic coil operated at radio frequency. After ignition with an initial electric spark, the free electrons are accelerated in the magnetic field and collide with the surrounding Ar atoms. The newly generated Ar ions and electrons are accelerated and produce cascading more electrons and ions. Within milliseconds, this generates a plasma with temperatures reaching up to 10,000 K. The sample is generally introduced to the plasma with a nebulizer for liquid samples, which generates a sample aerosol. This aerosol is easily evaporated, atomized and then ionized in the plasma by collision at the present temperature. Thereafter, the analyte ion is accelerated through the sampler and skimmer cone and focused with ion optics before being introduced to the mass analyzer. The mass analyzer of an ICP-MS is usually a quadrupole consisting of four parallel rods (ICP-QMS). An oscillating electrical field is applied, which creates helical flight paths for the passing ions. Through selective stabilization and destabilization of the flight path, only ions with a certain mass-to-charge ($m/z$) ratio can pass through the quadrupole. The potential of the rods can be changed rapidly, for the reason different $m/z$ ratios can be measured quasi-simultaneous in sequence. The passing ions are then converted, amplified and detected in a secondary electron multiplier. The intensity signal is proportional to the concentration in the sample solution. The ICP-MS technique is characterized by its simple

sample preparation, an atmospheric pressure ion source and simple quantification procedure with external standard solutions while showing excellent sensitivity, precision and accuracy. [108, 111]

As an alternative to a liquid sample introduction system by a nebulizer, solid samples can be introduced by LA. For the LA, a pulsed nanosecond laser beam is focused on the solid's surface. The local absorption of the laser's energy generates a small sample material plasma at the point of impact and the ablated material is transported by a transport gas such as He into the ICP. The time- and space-resolved ablation enables a detailed mapping of analytes in a solid sample. The advantage of a solid sample LA-ICP-MS is the direct measurement of a sample without possible influences and contamination from sample preparation. However, due to strong matrix influences during the ablation and quantification process, adapted reference materials need to be used, which are still rare, especially for organic matrices.[111] Since no suitable organic reference material was available for the measurement of silver within the mushroom fruit body cross-sections, an in-house standard of cellulose homogenized with a multi-element standard was developed. The homogeneity of the cellulose standard varied with different elements. **(D2)** [70]

In order to achieve better detection limits and eliminating of isobaric interferences several approaches were supplemented to an ICP-MS, e.g. collision/-reaction cells (CRC), time-of-flights ICP-TOF-MS, or single/multi ion collector double-focusing sector field (MC)-ICP-SFMS. Interferences can also be reduced by preceding separation techniques via high-performance liquid chromatography (HPLC) or capillary electrophoresis.[110, 111] The implementation of multipole CRC for ICP-QMS is one of the major improvements for the analysis of long-lived radionuclides by reducing interferences of stable isotopes, polyatomic species and peak tailing from abundant isotopes.[109–111] The CRC employs a combination of one or more different collision and reaction gases at different flow rates in the cell. Typical collision gases are He and $H_2$, whereas typical reaction gases are $O_2$, $NH_3$, $CH_4$ and $N_2O$. The collision gas is introduced to dissociate polyatomic interferences or plasma gas ions by energy transfer or collisional fragmentation. In contrast, collision with the reaction gas produces new interference free molecular shift ions. The reaction of the analyte with the reaction gas depends on its reaction thermochemistry and kinetics in the gas phase.[112] There are several design variants of CRC-ICP-QMS on the market. On one hand, the multipole CRC can be coupled with a subsequent quadrupole mass filter Q1. On the other hand, the CRC can be connected between two quadrupoles with mass filter Q1 and Q2. The advantages of the later ICP-MS/MS or ICP-QQQ-MS configuration is the preselection of the ions entering the CRC –suppressing unwanted secondary polyatomic interferences, and the improvement in abundance sensitivity in Q2.[112] As mentioned previously in Chapter 2.3.1 palladium shows a high affinity for organic molecules through bindings of carbon, oxygen and nitrogen. Chen *et al*. and Bandura *et al*. proposed the thermodynamic

favored biomolecular reaction of palladium ions with propane gas, whereas silver ions are not favored.[113, 114] In the publication (**D3**), the aforementioned bimolecular reaction was shown to be applicable to a commercial ICP-QQQ-MS instrument. The optimization of the CRC cell gas combination (Propane/He) and flow rates as well as instrument parameters allowed for a determination of palladium isotopes at the $C_2H_4^+$ shift (m/z:+28) at the same sensitivity as palladium without gas mode. The collision shifted palladium reduced the background significantly, even allowing the determination of ultra-traces of $^{107}Pd^+$ in presence of $^{107}Ag^+$ and $^{91}Zr^{16}O^+$ species in an environmental sample.[85]

## 2.6 Summary

A combination of various analytical methods and instrumentations were utilized during this work and allowed an accurate and precise measurement of ultra-traces of noble metal radionuclides. The radiosilver isotope $^{108m}Ag$ could be isolated from magnitudes higher amounts of concomitant $^{137}Cs$ via autodeposition and simple gamma spectrometric measurements. The use of autoradiography of $^{137}Cs$ and LA-ICP-MS measurements of stable silver $^{107}Ag$ and $^{109}Ag$ representative for $^{108m}Ag$ showed the ability of localization of contamination in self-grown shiitake mushrooms. Through isolation of palladium from a Chernobyl cooling pond sediment sample via cation-exchange resin, Ni Resin and ICP-QQQ-MS with CRC mode on propane/He gas, for a first time long-lived $^{107}Pd$ was determined with a high probability in the environment.

# Chapter 3

# Conclusion

The main focus of the dissertation was on the extraction, enrichment and isolation of noble metal radionuclides with a subsequent measurement on suitable radiometric or mass spectrometric instruments. For the extraction and isolation of the noble metal radionuclides, various aspects of analytical procedures were utilized. In this regard, preparation methods of an electrochemical nature such as autodeposition and extraction via selective resins allowed the enrichment and extraction of the noble metal radionuclides of interest. Subsequently, the isolated noble metal radionuclides were adapted to the measurement by radiometric and mass spectrometric instruments. The instrument of choice was selected according to the required sensitivity, the type of radiation, the half-life of the radionuclide and possible interferences.

In previous work, contaminations of radiosilver isotopes $^{108m}$Ag and $^{110m}$Ag were found in seafood samples from Japan. During the Fukushima Daiichi NPP accident on the 11$^{th}$ March 2011, the radionuclide $^{110m}$Ag was released in large quantities into the environment. As the Fukushima Daiichi NPP consisted of BWR units, the release of radiosilver was limited. However, in case of accidents in PWRs using control rods consisting of Ag-In-Cd alloy, the radiosilver isotopes $^{108m}$Ag and $^{110m}$Ag are going to be more prominent. The determination of radiosilver during the aftermath of a nuclear accident may also allow insight into the state of the control rods, pressure vessel sealings or other core components. During NPP accidental releases, the presence of other gamma emitters are omnipresent and will interfere with low-level-measurements of radiosilver. For this reason, the first publication **D1** focuses on the development of a separation protocol of radiosilver in the environment in presence of high contamination levels such as present during a nuclear accident. The determination of the noble metal radionuclides $^{108m}$Ag and $^{110m}$Ag in this scenario could give important information of the reactor conditions with focus on control rods of PWRs. For the analytical protocol simple autodeposition of silver on a copper plate and straightforward gamma spectrometry was chosen due to its simplicity and universal applicability with rapid results. The autodeposition showed an excellent separation efficiency of orders of magnitudes higher concentration of $^{137}$Cs in various aquatic media. The methods were also applicable for organic samples of paper **D1** after ashing and digestion sample preparation procedure. Another research topic addressed the fate of radiosilver and radiocesium in soil samples after a release scenario. For the soil study, two different soil types were contaminated with artificial salt solution of $^{108m}$Ag and $^{137}$Cs. One of the artificial salt solution represented typical $CaCl_2$ matrices, whereas the other consisted of $Ca(NO_3)_2$, which better represents agriculture areas. Fresh soil contamination shows for silver a high affinity to the residual fraction, whereas radiocesium has higher mobility. [47] It is known, that silver shows increased mobility in the presence of organic compounds in soil, which

might increase also its bioavailability. For radiation protection reasons, the information of possible bioaccumulation in organisms is of great importance.

In publication **D2**, a case study of the uptake and elemental distribution of radiosilver and radiocesium in Shiitake mushrooms was investigated. Mushroom are of special interest as a food source due to their high potential for bioaccumulation of various elements such as alkaline and heavy metals. They are already known for their accumulation of other radionuclides such as radiocesium. Also, the cultivation on sawdust substrate with its high organic content was of interest. For this study, Shiitake mushrooms were grown on $^{108m}$Ag and $^{137}$Cs contamination substrate incubated with shiitake mycelium. The subsequent analysis of the transfer factors was determined by gamma spectrometry. Radiocesium showed a bioaccumulation to the shiitake fruit body, whereas radiosilver was depleted. For further understanding of the bioaccumulation the elemental distribution of the radionuclide in the organism is essential. Due to the high activity of radiocesium present in the fruit bodies, the radiocesium distribution was detected with autoradiography, showing a strong enrichment in the hymenium. Due to the lower activity of radiosilver, LA-ICP-MS of stable silver isotopes was chosen for the localization of radiosilver in the fruit body. Silver was rather equally distributed in the fruit body with local enrichment in the mushroom stalks outer parts.[70] Low quantities of radiosilver were often interfered by other gamma emitters and needed sufficient separation to achieve low detection limits. On the contrary, the stable silver isotope $^{107}$Ag interferes with the difficult-to-measure noble metal radionuclide $^{107}$Pd. Palladium-107 is a pure beta-emitter with low beta energy and a long half-life, for which reason, radiometric methods reach their limit. The main focus of the third publication **D3** was on the development of an analytical protocol with subsequent mass spectrometric measurement via ICP-QQQ-MS for the long-lived $^{107}$Pd. Here, silver $^{107}$Ag plays an important role as the most crucial isobaric interference. The purpose of this analytical method was the measurement of sub-mBq·kg$^{-1}$ activity concentrations of the long-lived $^{107}$Pd in the environment, which has not been done before. To reduce interferences of several cations with focus of possible polyatomic and isobaric isotopes such as $^{88}$Y, $^{91}$Zr, $^{107}$Ag a combination of cation exchange and Ni Resin was employed. For a further reduction of interferences, the palladium isotopes were measured at a $C_2H_4^+$ shift (m/z=+28) with an ICP-QQQ-MS instrument with a propane/helium flux at the CRC. The methods were tested with stable palladium isotopes and showed detection limits comparable to the interference-free measurement of a palladium standard with the advantage of eliminating various interferences. Particularly noteworthy is that with this method $^{107}$Pd was detected with a high probability for the first time in the environment in a cooling pond sediment sample from Chernobyl NPP. [85]

# Chapter 4

# References

[1] IAEA, "Nuclear Fuel Cycle Information System: A Directory of Nuclear Fuel Cycle Facilities," 2009.

[2] O. Masson *et al.,* "Airborne concentrations and chemical considerations of radioactive ruthenium from an undeclared major nuclear release in 2017," *Proc. Natl. Acad. Sci. U.S.A*, 116, 34, 16750–16759, 2019, doi: 10.1073/pnas.1907571116.

[3] G. M. Mudd and M. Diesendorf, "Sustainability of uranium mining and milling: toward quantifying resources and eco-efficiency," *Environ. Sci. Technol.*, 42, 7, 2624–2630, 2008, doi: 10.1021/es702249v.

[4] G. Mudd, "Critical review of acid in situ leach uranium mining: 1. USA and Australia," *Environ. Geol.*, 41, 3-4, 390–403, 2001, doi: 10.1007/s002540100406.

[5] C. J. Hardy, "The chemistry of uranium milling," *Radiochim. Acta*, 25, 3/4, 121–134, 1978. Available: http://inis.iaea.org/search/search.aspx?orig_q=RN:10486807

[6] M. V. Glazoff, I. J. van Rooyen, B. D. Coryell, and C. J. Parga, "Comparison of Nuclear Fuels for TREAT: $UO_2$ vs $U_3O_8$," Idaho National Laboratory, INL/EXT-16-37972, 2016.

[7] United Nations Scientific Committee on the Effects of Atomic Radiation, Sources and effects of ionizing radiation: United Nations Scientific Committee on the Effects of Atomic Radiation UNSCEAR 2000 report to the General Assembly, with scientific annexes. New York: United Nations, 2000.

[8] P. Thakur, S. Ballard, and R. Nelson, "Radioactive fallout in the United States due to the Fukushima nuclear plant accident," *J. Environ. Monit.,* 14, 5, 1317–1324, 2012, doi: 10.1039/c2em11011c.

[9] International Atomic Energy Agency, "The International Nuclear and Radiological Event Scale User's Manual," 2013.

[10] W. B. Lewis, "The accident to the NRX reactor in December 12,1952," Atomic Energy of Canada Limited, Chalk River Project, Chalk River, Ontario.

[11] W. G. Cross, "The Chalk River accident in 1952," Atomic Energy of Canada Limited, Chalk River Nuclear Laboratorie*s,* Chalk River, Ontario.

[12] S. Jones, "Windscale and Kyshtym: a double anniversary," *J. Environ. Radioact.*, 99, 1, 1–6, 2008, doi: 10.1016/j.jenvrad.2007.10.002.

[13] A. V. Akleyev, L. Y. Krestinina, M. O. Degteva, and E. I. Tolstykh, "Consequences of the radiation accident at the Mayak production association in 1957 (the 'Kyshtym Accident')," *J. Radiol. Prot.*, 37, 3, R19-R42, 2017, doi: 10.1088/1361-6498/aa7f8d.

[14] E. K. Vasilenko, E. E. Aladova, M. V. Gorelov, V. A. Knyazev, D. V. Kolupaev, and S. A. Romanov, "The radiological environment at the Mayak PA site and

radiation doses to individuals involved in emergency and remediation operations after the 'Kyshtym Accident' in 1957," *J. Radiol. Prot.*, 40, 2, R23-R45, 2020, doi: 10.1088/1361-6498/ab8711.

[15] R. Querfeld *et al.,* "On the occurrence and origin of anthropogenic radionuclides found in a fragment of the Chelyabinsk (LL5) meteorite," *Meteorit. Planet. Sci.*, 52, 6, 1244–1250, 2017, doi: 10.1111/maps.12855.

[16] J. A. Garland and R. Wakeford, "Atmospheric emissions from the Windscale accident of October 1957," *Atmos. Environ.*, 41, 18, 3904–3920, 2007, doi: 10.1016/j.atmosenv.2006.12.049.

[17] D. W. Akers, R. K. Mccardell, M. L. Russell, and G. Worku, "TMI-2 Core materials and fission product inventory," *Nucl. Eng.Des.*, 118, 3, 451–461, 1990, doi: 10.1016/0029-5493(90)90046-Z.

[18] G. Steinhauser, A. Brandl, and T. E. Johnson, "Comparison of the Chernobyl and Fukushima nuclear accidents: a review of the environmental impacts," *Sci. Total Environ.*, 470-471, 800–817, 2014, doi: 10.1016/j.scitotenv.2013.10.029.

[19] S. Band *et al.,* "Fukushima Daiichi - Unfallablauf, radiologische Folgen: GRS-S-56," *GRS*, 5, 2016.

[20] F. Grünwald *et al.,* "Comparison of $^{18}$FDG-PET with $^{131}$Iodine and $^{99m}$Tc-Sestamibi Scintigraphy in Differentiated Thyroid Cancer," *Thyroid*, 7, 3, 1997.

[21] C. Hoehr *et al.,* "Medical Isotope Production at TRIUMF – from Imaging to Treatment," *Phys. Procedia*, 90, 200–208, 2017, doi: 10.1016/j.phpro.2017.09.059.

[22] T. Ruth, "Accelerating production of medical isotopes," *Nature*, 457, 7229, 536-7, 2009.

[23] C. Corkhill and N. Hyatt, Eds., Nuclear Waste Management: IOP Publishing, 2018.

[24] J. Tadmor, "Radioactivity from Coal-Fired Power Plants: A Review," *J. Environ. Radioact.*, 4, 177–204, 1986.

[25] C. Papastefanou, "Escaping radioactivity from coal-fired power plants (CPPs) due to coal burning and the associated hazards: a review," *J. Environ. Radioact.*, 101, 3, 191–200, 2010, doi: 10.1016/j.jenvrad.2009.11.006.

[26] G. Steinhauser, "Environmental nuclear forensics: the need for a new scientific discipline," *Environ. Sci. Pollut. Res. Int.*, 26, 17, 16901–16903, 2019, doi: 10.1007/s11356-019-04877-w.

[27] P. J. Coughtrey, F. W. Whicker, and V. Schultz, "Radioecology: Nuclear Energy and the Environment," *J. Appl. Ecol.*, 21,2, 733, 1984, doi: 10.2307/2403460.

[28] R. J. Pentreath, "Radioecology, radiobiology, and radiological protection: frameworks and fractures," *J. Environ. Radioact.*, 100, 12, 1019–1026, 2009, doi: 10.1016/j.jenvrad.2009.06.004.

[29] M. J. Kristo, "Nuclear forensics," in *Handbook of Radioactivity Analysis: Volume 2*: Elsevier, 2020, 921–951.

[30] K. Momma and F. Izumi, "VESTA 3 for three-dimensional visualization of crystal, volumetric and morphology data," *J. Appl. Crystallogr.*, 44, 6, 1272–1276, 2011, doi: 10.1107/S0021889811038970.

[31] $UO_2$ Crystal Structure: Datasheet from "PAULING FILE Multinaries Edition – 2012" in SpringerMaterials (https://materials.springer.com/isp/crystallographic/docs/sd_1819289): Springer-Verlag Berlin Heidelberg & Material Phases Data System (MPDS), Switzerland & National Institute for Materials Science (NIMS), Japan.

[32] R. C. Ewing, "Long-term storage of spent nuclear fuel," *Nat. Mater.*, 14, 3, 252–257, 2015, doi: 10.1038/nmat4226.

[33] F. Peiffer, B. McStocker, D. Gründler, F. Ewig, B. Thomauske, A.Havenith, J. Kettler, "Abfallspezifikation und Mengengerüst Basis Ausstieg Kernenergienutzung AP3," GRS-278

[34] G. Hirschberg *et al.,* "Accumulation of radioactive corrosion products on steel surfaces of VVER type nuclear reactors. I. [110m]Ag," *J. Nucl. Mater.*, 265, 3, 273–284, 1999, doi: 10.1016/S0022-3115(98)00656-4.

[35] D. Zok *et al.,* "Determination of Characteristic vs Anomalous [135]Cs/[137]Cs Isotopic Ratios in Radioactively Contaminated Environmental Samples," *Environ. Sci. Technol.*, 55, 8, 4984–4991, 2021, doi: 10.1021/acs.est.1c00180.

[36] P. R. J. Saey, T. W. Bowyer, and A. Ringbom, "Isotopic noble gas signatures released from medical isotope production facilities--simulations and measurements," *Appl. Radiat. Isot.*, 68, 9, 1846–1854, 2010, doi: 10.1016/j.apradiso.2010.04.014.

[37] T. Hopp, D. Zok, T. Kleine, and G. Steinhauser, "Non-natural ruthenium isotope ratios of the undeclared 2017 atmospheric release consistent with civilian nuclear activities," *Nat. Commun.*, 11, 1, 2744, 2020, doi: 10.1038/s41467-020-16316-3.

[38] J. Švedkauskaite-LeGore, K. Mayer, S. Millet, A. Nicholl, G. Rasmussen, and D. Baltrunas, "Investigation of the isotopic composition of lead and of trace elements concentrations in natural uranium materials as a signature in nuclear forensics," *Radiochim. Acta*, 95, 10, 2007, doi: 10.1524/ract.2007.95.10.601.

[39] K. Mayer, M. Wallenius, and I. Ray, "Nuclear forensics--a methodology providing clues on the origin of illicitly trafficked nuclear materials," *Analyst*, 130, 4, 433–441, 2005, doi: 10.1039/b412922a.

[40] J. M. Schwantes *et al.,* "Nuclear archeology in a bottle: evidence of pre-Trinity U.S. weapons activities from a waste burial site," *Anal. Chem.*, 81, 4, 1297–1306, 2009, doi: 10.1021/ac802286a.

[41] A. F. Holleman, Wiberg E., and N. Wiberg, Lehrbuch der Anorganischen Chemie, 102nd ed. Berlin, New York: Walter de Gruyter, 2007.

[42] M. Binnewies, Allgemeine und Anorganische Chemie, 2nd ed. Heidelberg, Neckar: Spektrum Akademischer Verlag, 2011.

[43] D. N. Sunderman and C. W. Townley, The Radiochemistry of Silver. Washington, D.C.: National Academies Press, 1961.

[44] J. J. Fritz, "Thermodynamic properties of chloro-complexes of silver chloride in aqueous solution," *J. Solut. Chem.*, 14, 12, 1985.

[45] I. Puigdomenech, "MEDUSA," 2010.

[46] A. Weller, M. Hori, K. Shozugawa, and G. Steinhauser, "Rapid ultra-trace determination of Fukushima-derived radionuclides in food," *Food Control*, 85, 376–384, 2018, doi: 10.1016/j.foodcont.2017.10.025.

[47] A. Weller, D. Zok, S. Reinhard, S. K. Woche, G. Guggenberger, and G. Steinhauser, "Separation of Ultratraces of Radiosilver from Radiocesium for Environmental Nuclear Forensics," *Anal. Chem.*, 92, 7, 5249–5257, 2020, doi: 10.1021/acs.analchem.9b05776.

[48] M. H. Lee, C. H. Lee, K. Song, C. K. Kim, and P. Martin, "Determination of Polonium Nuclides in a Water Sample with Solvent Extraction Method," *Bull. Korean Chem. Soc.*, 31, 9, 2488–2492, 2010, doi: 10.5012/bkcs.2010.31.9.2488.

[49] G. K. Schweitzer and J. W. Nehls, "Studies in Low Concentration Chemistry. II. The Radiocolloidal Properties of Silver-111," *J. Amer. Chem. Soc.*, 74, 1952.

[50] H. L. Hamester and M. Kahn, The adsorptive and radiocolloidal properties of carrier-free silver: Sandia Corporation, 1963.

[51] T. Kaiser and G. Wasserburg, "The isotopic composition and concentration of Ag in iron meteorites and the origin of exotic silver," *Geochim. Cosmochim. Acta*, 47, 1, 43–58, 1983, doi: 10.1016/0016-7037(83)90089-3.

[52] M. A. Wahlgren and W. W. Meinke, "Isomerism of Silver-108," *Phys. Rev.*, 118,. 1, 181–183, 1960, doi: 10.1103/PhysRev.118.181.

[53] J. Magill, G. Pfennig, R. Dreher, and Z. Sóti, Karlsruher Nuklidkarte: Chart of the nuclides, 9th ed. Eggenstein-Leopoldshafen, Germany: Nucleonica GmbH, 2015.

[54] D. A. Petti, "Silver-Indium-Cadmium Control Rod Behavior in Severe Reactor Accidents," *Nucl. Technol.*, 84, 2, 128–151, 1989, doi: 10.13182/NT89-A34183.

[55] R. Dubourg *et al.,* "Unterstanding the behaviour of absorber elements in silver-indium-cadmium control rods during PWR severe accident sequences: The 3rd European Review Meeting on Severe Accident Research (ERMSAR-2008)," Bulgaria, Sep. 2008.

[56] E. A. Lepel, Pratt, S.L., Robertson, D. E., C. W. Thomas, and D. L. Haggard, "Radiological characterization of spent control rod assemblies," *J. Radioanal. Nucl. Chem.*, 194, 1, 1995.

[57] I. Y. Emel'yanov, Y. I. Volod'ko, V. V. Postnikov, V. O. Steklov, and V. I. Uvarov, "Measurement of the sensitivity of neutron detectors with silver emitter during long service in reactor," *At. Energy*, 1977.

[58] D. R. Slaughter and W. L. Pickles, "A highly sensitive silver-activation detector for pulsed neutron sources," *Nucl. Instrum. Methods*, 160, 87–92, 1979.

[59] M. Yamazaki, Y. Tanizaki, and T. Shimokawa, "Silver and other trace elements in a freshwater fish, Carasius auratus langsdorfii, from the Asakawa River in Tokyo, Japan," *Environ. Pollut.*, 94, 1, 83–90, 1996, doi: 10.1016/S0269-7491(96)00053-X.

[60] R. Fukai and C. N.Murray, "Environmental behaviour of radiocobalt and radiosilver released from nuclear power stations into aquatic systems," *IAEA-SM-172/42*, 1973.

[61] T. M. Beasley and E. E. Held,"Silver-108m in Biota and Sediments at Bikini and Eniwetok Atolls," *Nature*, 230, 1971.

[62] X. Qiu *et al.,* "Pollution of radiocesium and radiosilver in wharf roach (Ligia sp.) by the Fukushima Dai-ichi Nuclear Power Plant accident," *J. Radioanal. Nucl. Chem.*, 311, 1, 121–126, 2017, doi: 10.1007/s10967-016-4879-1.

[63] A. Philippe and G. E. Schaumann, "Interactions of dissolved organic matter with natural and engineered inorganic colloids: a review," *Environ. Sci. Technol*, 48, 16, 8946–8962, 2014, doi: 10.1021/es502342r.

[64] A. A Pfau, R. Fischer, H. C. Heinrich and J. Handl, "Radiosilver [110m]Ag from Chernobyl and its transfer from plant to ruminants," *Proceedings of the XIXth ESNA-Conference*, 1988.

[65] Z. Vuković, "Environmental impact of radioactive silver released from nuclear power plant," *J. Radioanal. Nucl. Chem.*, 254, 3, 637–639, 2002.

[66] Z. Vuković, "Estimate of radio-silver release from chernobyl," *J. Environ. Radioact.*, 34, 2, 207–209, 1997, doi: 10.1016/0265-931X(96)00007-0.

[67] K. Maeda *et al.,* "Distribution of radioactive nuclides of boring core samples extracted from concrete structures of reactor buildings in the Fukushima Daiichi Nuclear Power Plant," *J. Nucl. Sci. Technol.*, 51, 7-8, 1006–1023, 2014, doi: 10.1080/00223131.2014.915769.

[68] H. Lepage *et al.,* "Environmental mobility of [110m]Ag: lessons learnt from Fukushima accident (Japan) and potential use for tracking the dispersion of contamination within coastal catchments," *J. Environ. Radioact.*, 130, 44–55, 2014, doi: 10.1016/j.jenvrad.2013.12.011.

[69] G. Szabó, J. Guczi, J. Valyon, and R. A. Bulman, "Investigations of the sorption characteristics of radiosilver on some natural and artificial soil particles," *Sci. Total Environ.*, 172, 1, 65–78, 1995, doi: 10.1016/0048-9697(95)04781-6.

[70] A. Weller, D. Zok, and G. Steinhauser, "Uptake and elemental distribution of radiosilver [108m]Ag and radiocesium ^{137}Cs in shiitake mushrooms (*Lentinula edodes*)," *J. Radioanal. Nucl. Chem.*, 322, 3, 1761–1769, 2019, doi: 10.1007/s10967-019-06778-1.

[71] G. Bystrzejewska-Piotrowska, D. Pianka, M. A. Bazała, R. Steborowski, J. L. Manjón, and P. L. Urban, "Pilot study of bioaccumulation and distribution of cesium, potassium, sodium and calcium in king oyster mushroom (Pleurotus

eryngii) grown under controlled conditions," *Int. J. Phytoremediation*, 10, 6, 503–514, 2008, doi: 10.1080/15226510802114987.

[72] O. Isildak, I. Turkekul, M. Elmastas, and H. Y. Aboul-Enein, "Bioaccumulation of Heavy Metals in Some Wild-Grown Edible Mushrooms," *Anal. Lett,* 40, 6, 1099–1116, 2007, doi: 10.1080/00032710701297042.

[73] A. Demirbas, "Heavy metal bioaccumulation by mushrooms from artificially fortified soils," *Food Chem.,* 71, 293–301, 2001.

[74] O. T. Hogdahl, The radiochemistry of palladium. Washington, D.C.: National Academies Press, 1961.

[75] C. Colombo, Oates C. J., A. J. Monhemius, and J. A. Plamt, "Complexation of platinum, palladium and rhodium with inorganic ligands in the environment," *Geochem. Explor. Env. A*, 8, 1–11, 2008.

[76] J. Tsuji, "Carbon-carbon bond formation via palladium complexes," *Acc. Chem. Res.*, 2, 144–152, 1969.

[77] N. Miyaura, Ed., *Cross-Coupling Reactions.* Berlin, Heidelberg: Springer Berlin Heidelberg, 2002.

[78] L. Yin and J. Liebscher, "Carbon-carbon coupling reactions catalyzed by heterogeneous palladium catalysts," *Chem. Rev*, 107, 1, 133–173, 2007, doi: 10.1021/cr0505674.

[79] S. Asai *et al.,* "Determination of $^{107}$Pd in Pd Recovered by Laser-Induced Photoreduction with Inductively Coupled Plasma Mass Spectrometry," *Anal. Chem.*, 88, 24, 12227–12233, 2016, doi: 10.1021/acs.analchem.6b03286.

[80] R. Aono *et al.,* "Development of $^{93}$Zr, $^{93}$Mo, $^{107}$Pd and $^{126}$Sn Analytical Methods for radioactive Waste from Fukushima Daiichi Nuclear Power Station," *JAEA Technology*, 2017-025, 2017.

[81] S. Dulanská, B. Horváthová, B. Remenec, and Ľ. Mátel, "Determination of $^{107}$Pd in radwaste using Ni Resin," *J. Radioanal. Nucl. Chem.*, 310, 2, 645–650, 2016, doi: 10.1007/s10967-016-4827-0.

[82] B. Andris, M. Pražský, and F. Šebesta, "Rapid separation and determination of $^{107}$Pd in radioactive waste produced during NPP A-1 decommissioning," *J. Radioanal. Nucl. Chem.*, 304, 1, 123–126, 2015, doi: 10.1007/s10967-014-3707-8.

[83] T. Yomogida *et al.,* "Non-contact and Selective Pd Separation Based on Laser-induced Photoreduction for Determination of $^{107}$Pd by ICP-MS —The Relation between Separation Conditions and Pd Rsecovery—," *Bunseki Kagaku*, 66, 9, 647–652, 2017, doi: 10.2116/bunsekikagaku.66.647.

[84] M. Bertaux *et al.,* "Analytical improvements for long-lived radionuclides determination in zircaloy hulls," *Atalante*, Montepellier (France), 2008.

[85] A. Weller *et al.,* "Detection of the Fission Product Palladium-107 in a Pond Sediment Sample from Chernobyl," *Environ. Sci. Technol. Lett.*, 8, 8, 656-661, 2021, doi: 10.1021/acs.estlett.1c00420.

[86] F. Zereini and F. Alt, Palladium emissions in the environment: Analytical methods, environmental assessment and health effects. Berlin, New York: Springer, 2006.

[87] G. H. Rizvi, J. N. Mathur, M. S. Murali, and R. H. Iyer, "Recovery of Fission Product Palladium from Acidic High Level Waste Solutions," *Sep. Sci. Technol.*, 31, 13, 1805–1816, 1996, doi: 10.1080/01496399608001011.

[88] M. Zha, J. Liu, Y.-L. Wong, and Z. Xu, "Extraction of palladium from nuclear waste-like acidic solutions by a metal–organic framework with sulfur and alkene functions," *J. Mater. Chem. A*, 3, 7, 3928–3934, 2015, doi: 10.1039/C4TA06678B.

[89] Y. Liu *et al.,* "Variation in palladium and water quality parameters and their relationship in the urban water environment," *Water Sci. Technol.*, 81, 11, 2450–2458, 2020, doi: 10.2166/wst.2020.303.

[90] B. Sures, S. Zimmermann, J. Messerschmidt, and A. von Bohlen, "Relevance and Analysis of Traffic Related Platinum Group Metals(Pt, Pd, Rh) in the Aquatic Biosphere, with Emphasis on Palladium," *Ecotoxicology*, 11, 385–392, 2002.

[91] S. A. Wood and J. Middlesworth, "The influence of acetate and oxalate as simple organic ligands on the behaviour of palladium in surface environments," *Canad. Mineral.*, 42, 411–421, 2004.

[92] F. Zereini, C. L. S. Wiseman, J. Poprizki, P. Albers, W. Schneider, and K. Leopold, "Assessing the potential of inorganic anions ($Cl^-$, $NO_3^-$, $SO_4^{2-}$ and $PO_4^{3-}$) to increase the bioaccessibility of emitted palladium in the environment: Experimental studies with soils and a Pd model substance," *Environ. Pollut.*, 220, Pt B, 1050–1058, 2017, doi: 10.1016/j.envpol.2016.11.039.

[93] D. Fatta-Kassinos, K. Bester, and K. Kümmerer, *Xenobiotics in the Urban Water Cycle*. Dordrecht: Springer Netherlands, 2010.

[94] C. Colombo, A. J. Monhemius, and J. A. Plant, "The estimation of the bioavailabilities of platinum, palladium and rhodium in vehicle exhaust catalysts and road dusts using a physiologically based extraction test," *Sci. Total Environ.*, 389, 1, 46–51, 2008, doi: 10.1016/j.scitotenv.2007.08.022.

[95] C. L. S. Wiseman and F. Zereini, "Airborne particulate matter, platinum group elements and human health: a review of recent evidence," *Sci. Total Environ.*, 407, 8, 2493–2500, 2009, doi: 10.1016/j.scitotenv.2008.12.057.

[96] K. M. Matthews, "The CTBT-verification significance of particulate radionuclides detected by the International Monitoring System," *National Radiation Laboratory*, 2005.

[97] S. G. Bratsch, "Standard Electrode Potentials and Temperature Coefficients in Water at 298.15 K," *J. Phys. Chem. Ref. Data*, 18, 1, 1–21, 1989, doi: 10.1063/1.555839.

[98] T. Li *et al.,* "TEM observation of general growth behavior for silver electroplating on copper rod," *Appl. Surf. Sci.*, 451, 148–154, 2018, doi: 10.1016/j.apsusc.2018.04.260.

[99] X. Xu, X. Luo, H. Zhuang, W. Li, and B. Zhang, "Electroless silver coating on fine copper powder and its effects on oxidation resistance," *Mater. Lett.*, 57, 24-25, 3987–3991, 2003, doi: 10.1016/S0167-577X(03)00252-0.

[100] X. Dai and S. Kramer-Tremblay, "Five-column chromatography separation for simultaneous determination of hard-to-detect radionuclides in water and swipe samples," *Anal. Chem.*, 86, 11, 5441–5447, 2014, doi: 10.1021/ac500572g.

[101] L. E. Jassin, "Radiochemical separation advancements using extraction chromatography: A review of recent Eichrom sers' Group Workshop presentations with a focus on matrix interferences," *J. Radioana. Nucl. Chem.*, 263, 1, 93–96, 2005.

[102] C. Testa and A. Delle Site, "The application of extraction chromatography to the determination of radionuclides in biological and environmental samples," *J. Radioanal. Nucl. Chem.*, 34, 1, 121–134, 1976, doi: 10.1007/BF02521514.

[103] A. Zulauf, S. Happel, M. B. Mokili, A. Bombard, and H. Jungclas, "Characterization of an extraction chromatographic resin for the separation and determination of 36Cl and 129I," *J. Radioanal. Nucl. Chem.*, 286, 2, 539–546, 2010, doi: 10.1007/s10967-010-0772-5.

[104] Triskem International, "TBP resin: product sheet and literature study," 2015.

[105] A. S. J. Reis, E. S. C. Temba, G. F. Kastner, and R. P. G. Monteiro, Radiochemical Separation of Nickel for $^{59}$Ni and $^{63}$Ni Activity Determination in Nuclear Waste Samples: InTech, 2012.

[106] S. Rajkovich, D. Chahill, L. Peedin, and S. Wheland, "2 Case Studies Using Eichrom's Nickel Resin: A Nuclear Power Plant and a Commercial Laboratory: RS196," Cincinnati, 1996.

[107] J.-V. Kratz and K. H. Lieser, Nuclear and radiochemistry: Fundamentals and applications. Weinheim: Wiley-VCH.

[108] X. Hou and P. Roos, "Critical comparison of radiometric and mass spectrometric methods for the determination of radionuclides in environmental, biological and nuclear waste samples," *Anal. Chim. Acta*, 608, 2, 105–139, 2008, doi: 10.1016/j.aca.2007.12.012.

[109] I. W. Croudace, B. C. Russell, and P. W. Warwick, "Plasma source mass spectrometry for radioactive waste characterisation in support of nuclear decommissioning: a review," *J. Anal. At. Spectrom.*, 32, 3, 494–526, 2017, doi: 10.1039/C6JA00334F.

[110] P. E. Warwick, B. C. Russell, I. W. Croudace, and Ž. Zacharauskas, "Evaluation of inductively coupled plasma tandem mass spectrometry for radionuclide assay in nuclear waste characterisation," *J. Anal. At. Spectrom.*, 34, 9, 1810–1821, 2019, doi: 10.1039/C8JA00411K.

[111] J. S. Becker, "Mass spectrometry of long-lived radionuclides," *Spectrochim. Acta B*, 58, 10, 1757–1784, 2003, doi: 10.1016/S0584-8547(03)00156-3.

[112] S. D. Tanner, V. I. Baranov, and D. R. Bandura, "Reaction cells and collision cells for ICP-MS: a tutorial review," *Spectrochim. Acta B*, 57, 1361–1452, 2002.

[113] Y.-M. Chen, M. R. Sievers, and P. B. Armentrout, "Activation of $CH_4$, $C_2H_6$, $C_3H_8$, and c-$C_3H_6$ by gas-phase $Pd^+$ and the thermochemistry of Pd-ligand complexes," *Int. J. Mass Spectrom. Ion Processes*, 167/168, 195–212, 1997.

[114] D. R. Bandura, V. I. Baranov, A. E. Litherland, and S. D. Tanner, "Gas-phase ion–molecule reactions for resolution of atomic isobars: AMS and ICP-MS perspectives," *Int. J. Mass Spectrom.*, 255-256, 312–327, 2006, doi: 10.1016/j.ijms.2006.06.012.

Chapter 5

Publication D1

# Separation of Ultratraces of Radiosilver from Radiocesium for Environmental Nuclear Forensics

A. Weller, D. Zok, S. Reinhard, S. K. Woche, G. Guggenberger, G. Steinhauser

Author's contribution:

AW, DZ and GS designed the study

AW, DZ, SR have performed the laboratory experiments

SW carried out the surface analysis via SEM-EDX and XPS and evaluated the data

AW; GG and GS discussed the results

AW and GS contributed to the writing of the manuscript

# Chapter 6

## Publication D2

## Uptake and elemental distribution of radiosilver $^{108m}$Ag and radiocesium $^{137}$Cs in shiitake mushrooms (*Lentinula edodes*)

A. Weller, D. Zok, G. Steinhauser

Author's contribution:

AW and GS designed the study

AW performed the laboratory experiments and the autoradiography

AW and DZ conducted the LA-ICP-MS measurement

AW and GS contributed to the writing of the manuscript

# Chapter 7

# Publication D3

# Detection of the Fission Product Palladium-107 in a Pond Sediment Sample from Chernobyl

A. Weller, T. Ramaker, F. Stäger, T. Blenke, M. Raiwa, I. Chyzhevskyi, Serhii Kirieiev, S. Dubchak, G. Steinhauser

Author's contribution:

AW and GS designed the study

AW has performed the laboratory experiments and measurements and guided TR, FS, TB and MR in the experiments

TB, IC, SK; SD, GS performed the sampling campaign

AW, TR and GS discussed the results

AW and GS contributed to the writing of the manuscript

# Appendix

## Curriculum Vitae

| Name | Anica Weller |
| --- | --- |
| Geburtsdatum | 15.04.1992 in Delmenhorst |

## Ausbildung

| 2017-2021 | Promotion am Institut für Radioökologie und Strahlenschutz an der Leibniz Universität Hannover mit Förderung durch das Promotionsstipendium der Deutschen Bundesstiftung Umwelt (DBU) |
| --- | --- |
| 2014-2017 | Masterstudium Analytik, Leibniz Universität Hannover |
| 2011-2014 | Bachelorstudium Chemie, Leibniz Universität Hannover |

## Wissenschaftliche Publikationen

A. Weller, T. Ramaker, F. Stäger, T. Blenke, M. Raiwa, Ihor Chyzhevskyi, Serhii Kirieiev, Sergiy Dubchak, G. Steinhauser; Detection of the fission product Palladium-107 in a pond sediment sample from Chernobyl, *Environ. Sci. Technol. Lett*. In Press; DOI: 10.1021/acs.estlett.1c00420

R. Querfeld, M. Hori, A. Weller, K. Shozugawa, G. Steinhauser, Radioactive games? Radiation hazard assessment of the Tokyo Olympic summer games, *Environ. Sci. Technol.,* 2020, 54(18), 11414-11423. DOI: 10.1021/acs.est.0c02754

A. Weller, D. Zok, S. Reinhard, S. K. Woche, G. Guggenberger, G. Steinhauser; Separation of Ultratraces of Radiosilver from Radiocesium for Environmental Nuclear Forensics, *Anal. Chem.*, 2020, 92, 5249-5257. DOI: 10.1021/acs.analchem.9b05776

A. Weller, D. Zok, G. Steinhauser; Uptake and elemental distribution of radiosilver $^{108m}$Ag and radiocesium $^{137}$Cs in shiitake mushrooms (*Lentinula edodes*), *J. Radioanal. Nucl. Chem.*, 2019, 322 (3), 1761-1769. DOI: 10.1007/s10967-019-06778-1

F. Köhler, B. Riebe, A. Weller, C. Walther; Determination of iodine mobility in the soil vadose zone using long-term column experiments, *J. Radioanal. Nucl. Chem.*, 2019, 322 (3), 1755-1760. DOI: 10.1007/s10967-019-06789-y

O. Masson, G. Steinhauser, D. Zok, O. Saunier, H. Angelov, D. Babić, V. Bečková, J. Bieringer, M. Bruggeman, C.I. Burbidge, S. Conil, A. Dalheimer, L.-E. De Geer, A. de Vismes Ott, K. Eleftheriadis, S. Estier, H. Fischer, M.G. Garavaglia, C. Gasco Leonarte, K. Gorzkiewicz, D. Hainz, I. Hoffman, M. Hýža, K. Isajenko, T. Karhunen, J. Kastlander, C. Katzlberger, R. Kierepko, G.-J. Knetsch, J. Kövendiné Kónyi, M. Lecomte, J.W. Mietelski, P. Min, B. Møller, S.P. Nielsen, J. Nikolic, .L Nikolovska, I. Penev, B. Petrinec, P.P. Povinec, R. Querfeld, O. Raimondi, D. Ransby, W. Ringer, O. Romanenko, R. Rusconi, P.R.J. Saey, V. Samsonov, B. Šilobritienė, E. Simion, C. Söderström, M. Šoštarić, T. Steinkopff, P. Steinmann, I. Sýkora, L. Tabachnyi, D. Todorovic, E. Tomankiewicz, J. Tschiersch, R. Tsibranski, M. Tzortzis, K. Ungar, A. Vidic, A. Weller, H. Wershofen, P. Zagyvai, T. Zalewska, D. Zapata García, B. Zorko; Airborne concentrations and chemical considerations of radioactive ruthenium from an undeclared major nuclear release in 2017, *Proc. Natl. Acad. Sci. USA*, 2019, 116 (34), 16750-16759. DOI: 10.1073/pnas.1907571116

A. Weller, R. Querfeld, F. Köhler, G. Steinhauser; Aspects of quality assurance and performance of strontium-selective resins under non-routine conditions: old resins, delayed elution, *J. Radioanal. Nucl. Chem.*, 2019, 320 (2), 467-474. DOI: 10.1007/s10967-019-06484-y

R. Himstedt, D. Hinrichs, J. Sann, A. Weller, G. Steinhauser, D. Dorfs; Halide ion influence on the formation of nickel nanoparticles and their conversion into hollow nickel phosphide and sulhide nanocrystals, *Nanoscale*, 2019 11 (32), 15104-15111. DOI: 10.1039/C9NR04187G

A. Weller, M. Hori, K. Shozugawa, G. Steinhauser; Rapid ultra-trace determination of Fukushima-derived radionuclides in food, *Food Control*, 2018, 85, 376-384, DOI: 10.1016/j.foodcont.2017.10.025

A. Weller, E. J. Carrasco-Correa, C. Belenguer-Sapiña, A. de los Reyes Mauri-Aucejo, P. Amorós, J. M. Herrero-Martínez; Organo-silica hybrid capillary monolithic column with mesoporous silica particles for separation of small aromatic molecules, *Microchim. Acta,* 2017, 184 (10, 3799-3808. DOI: 10.1007/s00604-017-2404-z

Selbständigkeitserklärung

Hiermit versichere ich, dass die vorliegende Dissertation selbstständig verfasst und keine anderen als die angegebenen Quellen und Hilfsmittel verwendet wurden. Alle Stellen der Dissertation, die wörtlich oder sinngemäß aus anderen Quellen übernommen wurden, sind als solche kenntlich gemacht. Tabellen und Abbildungen, die nicht mit einer Quelle gekennzeichnet sind, wurden selbst erstellt. Ferner versichere ich, dass die vorliegende Dissertation noch nicht als Prüfungsarbeit für andere Prüfungen eingereicht worden ist.


Braunschweig, 26.08.2021


_____

(Anica Weller)